PHYSIOLOGICAL REVIEWS
Vol. 65, No. 1, January 1985
Printed in U.S.A.

Current Source-Density Method and Application in Cat Cerebral Cortex: Investigation of Evoked Potentials and EEG Phenomena

U. MITZDORF

Institut für Medizinische Psychologie, Ludwig-Maximilians-Universität München, Munich, West Germany

I. INTRODUCTION

The first methodical tool used in the pioneering works of neurophysiology was the recording of mass action potentials, i.e., the electroencephalogram (EEG) and cortical evoked potentials (12, 14). As soon as the technical development made the registration of potentials with high-resistance microelectrodes possible, however, neurophysiological research concentrated on the investigation of single-unit properties (2). Mass action potentials (APs) were progressively more neglected in basic research. They were pushed toward empiricism. The purely phenomenological application of the EEG in clinical diagnosis is the most prominent example.

0031-9333/85 **$1.50** Copyright © 1985 the American Physiological Society

The reason for this change is obvious: field potentials, although easy to record, are difficult to interpret. They are indirect and ambiguous reflections of the underlying neuronal activities. Action potentials, on the other hand, are clearly identified as the unique output signals of single units (e.g., refs. 19, 303). The concentration on single-unit investigations was justified and consolidated by successes. In sensory physiology, for example, this method proved to be adequate for studying the first steps of afferent information processing (119, 146, 160, 205).

This tool, however, not only contains the drawbacks of arbitrariness in selecting different cell types (see ref. 293) and the necessity for unmanageable sample sizes for answering more complex questions, it also incorporates a conceptual shortcoming: due to the prevalence of single-unit studies, current knowledge is biased toward single-cell functions. The receptive-field properties of single units, however, appear to be the dominant aspect of information processing only up to the first intracortical relay station (185, 302). From there, more subtle delocalized interaction phenomena, which are barely accessible to single-unit studies could dominate (e.g., refs. 58, 137, 238, 288).

Therefore it seems appropriate to again concentrate on the investigation of mass actions. In addition to the newly developed metabolism-related methods (274, 283), anatomical tracing methods (33), and histochemical methods (53), the recording of field potentials is also an appropriate tool for study of ensemble properties of neuronal masses (e.g., ref. 77).

By analogy with other macro-description methods (261), the promise of field-potential research is twofold. *1*) It may disclose interaction phenomena that are not accessible to single-unit studies and may thereby help to understand higher stages of intracortical information processing. *2*) By combining field-potential data with anatomical and single-unit results, it may also be possible to bridge the gap between the micro-description at the single-unit level and the macro-description at the field-potential level.

When studying neuronal mass actions via field potentials, submitting the original data to current source-density (CSD) analysis has proven very helpful. This method gives direct access to the physiologically relevant information, which is often concealed in the original data. It reveals the current sinks and sources in the extracellular space. These are, on one hand, the local generators of the field potentials. On the other hand, they are caused by the activation of neuronal ensembles. Therefore they are the link between the field potentials and the neuronal activities (Fig. 1). These causal relationships became manifest around 1950 (48). At the same time, Pitts (232) formulated the CSD method. However, broad acceptance of this method as an appropriate tool in field-potential studies started only 20 years later.

The essential features of the CSD method, as well as the basic arguments for interpreting its results, are reviewed in section II. Most of the studies that applied the CSD method are briefly considered. In section III, one specific attempt to reveal complementary information from field potentials, and to relate them to the underlying single-unit activity is outlined. It is based on

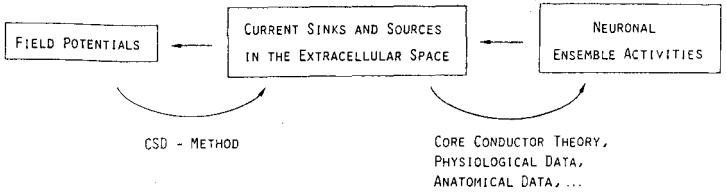

FIG. 1. *Straight arrows* represent causal relationships between field potentials, current source densities (CSDs), and neuronal activities; *curved arrows* represent techniques required to understand these causal relationships.

CSD data from the cat visual cortex. This specific example has been selected to illustrate the theoretical considerations, because the extraordinary wealth of anatomical and physiological facts known about this area allowed CSDs and neuronal activities to be related in great detail (Fig. 1). Analogous studies of the pericruciate cortex, as well as a generalization of the findings from CSDs about the intracortical processing of primary afferent information is discussed in section IV. Section V includes the relationships between EEG phenomena and intracortical CSDs and their similarities with primary evoked cortical activity. Finally, in section VI the central aspects of the CSD method as a complement to anatomical and single-unit methods is summarized (VI*A*), and the uniformity of cortical activation as revealed by the comparison of different types of field potentials is stressed (VI*B*).

II. CURRENT SOURCE-DENSITY (CSD) METHOD

During all types of neuronal activity, currents flow through the cell membranes. Viewed from the extracellular space on a macroscopic scale, these membrane currents are sinks (inward currents) and sources (outward currents). These sinks and sources are the physical causes of the field potentials (see Fig. 1).

The sink and source distributions can be calculated from the field potentials by the CSD method. Although this procedure does not reveal any new information, it is an essential step; in analogy to discrete localized charges versus their dissipated, superimposed potential fields in electrostatics, the sinks and sources, in contrast with the field potentials, are spatially localized phenomena. Therefore, the CSD method leads to a far higher spatial resolution of events.

A. Physical and Physiological Basis

Since several detailed derivations of the CSD method with thorough considerations of the inherent assumptions have been published (68, 101, 118, 216, 218, 219), only the basic ideas of this method are outlined here.

To a good approximation, the extracellular space can be considered independent of the intracellular space, because its boundaries, the cell membranes, have high resistances (several $k\Omega \cdot cm^2$), compared with the resistance of the extracellular space ($\sim$200 $\Omega \cdot$ cm). Due to neuronal activity, currents flow through these membranes into and out of the extracellular space. In the physical sense, these membrane currents are the boundary conditions for the description of the extracellular space (Laplace equation; 126).

However, the details at this microscopic level are not accessible via the macroscopic field potentials. The macroscopic level is reached by volume averaging of the individual microscopic membrane currents, resulting in the CSD (I_m; a scalar quantity of dimension A/cm^3). Due to the continuity of the current, this volume average of the membrane current density ($\vec{J}_m$) is equivalent to the divergence of the extracellular current density $\vec{J}$ (216, 219, 246)

$$\vec{\nabla} \cdot \vec{J} = I_m \tag{1}$$

If the outward currents dominate in a volume element, a current source results ($I_m > 0$); if the inward currents dominate, a current sink results ($I_m < 0$). The membrane currents that actually flow may be much larger than the fraction manifest in the current sinks and sources after the averaging procedure; but this averaging is inherent in the field potentials (ϕ) as well.

Within the range of frequencies of physiological interest (0–1 kHz), capacitive, inductive, magnetic, and propagative effects of the bioelectrical signals in the extracellular space can be neglected (69, 233). The error induced by these assumptions, essentially due to a small capacitive component, is <10% (23, 68, 218, 221, 233, 247, 248). This allows the quasi-static description of the electric field ($\vec{E}$) in the extracellular space and implies the validity of Ohm's law (233)

$$\vec{J} = \sigma \cdot \vec{E} \tag{2}$$

where σ is the conductivity tensor. $\vec{E}$ can be substituted by the gradient of the scalar potential (ϕ)

$$\vec{E} = -\vec{\nabla}\phi \tag{3}$$

leading to a linear relation between the current density and the gradient of the field potential in the extracellular space

$$\vec{J} = -\sigma \cdot \vec{\nabla}\phi \tag{4}$$

By elimination of $\vec{J}$ from *Equations 1* and *4*, the Poisson equation for the continuous source distribution I_m results (126)

The geometric (anatomical) properties of the neuronal tissue are inherent in the conductivity tensor. They define the optimal coordinate system, which reduces the conductivity tensor to its three main components (216). In all applications until now, the rectangular cartesian coordinate system was chosen. Thereby the effects of the curvatures of laminated structures were neglected (see ref. 101). In optimally oriented cartesian coordinates, *Equation 5* becomes

$$\sum_{i=1}^{3} \left(\frac{\partial \sigma_{ii}}{\partial x_i} \cdot \frac{\partial \phi}{\partial x_i} + \sigma_{ii} \cdot \frac{\partial^2 \phi}{\partial x_i^2} \right) = -I_m \tag{6}$$

where $x \equiv x_1$, $y \equiv x_2$, $z \equiv x_3$ and $\sigma_x \equiv \sigma_{11}$, $\sigma_y \equiv \sigma_{22}$, $\sigma_z \equiv \sigma_{33}$ (218).

If the medium is anisotropic, the three components of the conductivity tensor have different values. In fact, due to the alignment of elongated processes (fiber bundles or dendrites), most neuronal tissues are anisotropic (68, 111, 218, 248, 324).

If the medium is inhomogeneous, the values for the components of the conductivity tensor differ at different locations. This property of tissue is crucial even for qualitative estimates of CSD distributions, due to the terms containing the conductivity gradient in *Equation 6*. Experimentally, however, this property is difficult to assess [even if the principal problem of passive current flow through neurons is ignored (81)]. Results from different laboratories diverge, and the reported scatters of the values are high (23, 70, 101, 104, 111, 192, 218, 224, 251, 313, 324). In the cat cortex two studies revealed homogeneity through all layers (70, 192); in one study a significant conductivity increase was found in layer I (111). At least with the exception of layer I, homogeneity can therefore be assumed in the cat cortex.

In laminated structures that are activated homogeneously with respect to the laminar planes, the field potential is translationally invariant in the two directions parallel to the laminar planes (67, 101, 295). [Boundary effects due to focal activations have been investigated theoretically by Nicholson and Freeman (218).] In these situations the one-dimensional CSD method can be applied. Including anatomical homogeneity, *Equation 6* is reduced to

$$\sigma_z \cdot \frac{\partial^2 \phi}{\partial z^2} = -I_m \tag{7}$$

where z is the direction perpendicular to the laminae.

This is the simplest form of the CSD method. It can easily be conceived intuitively: according to Ohm's law, the steeper the potential gradient, the more current flows. Changes in the potential gradient ($\equiv \partial^2\phi/\partial z^2$) therefore imply changes in the amount of current flowing. As the extracellular space is a purely passive medium, increases and decreases in current flow must be due to membrane currents that enter or leave, respectively, the extracellular

demonstrated by localizing artificially produced sinks and sources in the cerebellar and cerebral cortices *(68, 192, 218)*.

Experimentally, the profiles of field potentials are obtained by measurements at discrete equidistant locations, and the second spatial derivative is calculated according to a finite difference formula *(66)*. Most commonly, the second spatial derivative is approximated by

$$\frac{\partial^2 \phi}{\partial z^2} \approx \frac{\phi(z + n \cdot \Delta z) - 2\phi(z) + \phi(z - n \cdot Az)}{(n \cdot \Delta z)^2} \qquad (8)$$

where Az is the distance between adjacent recording sites and $n \cdot Az$ is the differentiation grid (usually $n = 1$ or 2). The optimal choice of the differentiation grid depends on the anatomical order of the structure and can be judged from the shape of the potential profile, i.e., the dominant spatial frequency components of the potential *(66, 196)*.

Because total inward and outward membrane currents are equal in amplitude in the physiological situations considered here (see sect. II*C*), monopoles (i.e., imbalanced sinks or sources) can be excluded as possible generators of field potentials. Two types of generators may occur in principle (for details see sect. II*C*). *1)* Sink/source dipoles (or sheets of dipoles) generate a potential field that is positive in the region of the source, negative in the region of the sink, and zero on the equidistant plane between. Beyond the CSD distribution this potential decays only slowly. The limit values for this decay are $\phi \propto 1/z^2$ for one dipole and ϕ = constant (!) for an infinitely extended sheet. This potential field outside the CSD distribution is termed *far field (178)*. ***2)*** Symmetrical arrangements, like a source/sink/source distribution, generate a *closedfield* (178), which is large at the location of the central part of the CSD and decays to zero toward the borders of the CSD This type of potential does not reverse in sign and does not have a far-field component.

In general, the reverse of the CSD analysis is not possible; i.e., field potentials cannot be calculated from CSDs. The CSD analysis reveals the local causes of the field potentials and thereby eliminates far-field contributions. The knowledge of these far fields would be necessary, however, to reconstruct the field potentials from the CSDs.

B. *Experimental CSD Studies*

The CSD method has been applied for analysis of electrically evoked potentials *(3, 28, 61, 64–68, 101, 102, 118, 122,* 140a, *141, 161,* 186a, *195–200, 217, 220, 232, 272, 277, 295, 306, 312, 313,* 317), adequately evoked potentials *(23, 65, 67, 103, 104, 112, 143, 183, 193, 194, 208, 211, 214, 251, 278,* 314), and pathological events *(116, 231, 235, 251, 268, 306)*. It has been used to study ensemble activities in the spinal cord *(118,* 232), the medulla oblongata (141), a thalamic nucleus *(195, 196,* 199), tectal structures *(28, 64, 65, 67,* 186a, *208,*

295, 312, 313), the hippocampal formation (3, 102, 161, 272, 317), the cerebellum *(66, 68, 217,* 220), the prepyriform cortex (101), the neocortex *(61, 112, 116,* 122, 140a, *143, 183, 192, 194, 197–200, 208, 211, 231, 235, 251, 252, 268, 277, 278, 306,* 314), the retina *(103, 104,* 214), and the acoustic neuropil of an insect *(23)*.

The analyses were performed in various degrees of complexity. In several studies the one-dimensional approximation was applied at discrete times to yield the CSD distribution related to a certain potential peak *(3, 28, 61,* 101–*104, 122, 214, 235, 268, 312)*. In most applications, one-dimensional CSD profiles as continuous functions of time were evaluated *(64, 66–68,* 140a, *143, 183,* 186a, *193–200, 208, 211, 231, 251, 252, 272, 277, 278, 295, 306, 313,* 314). In four studies, including the two pioneering works, two-dimensional CSD distributions were calculated *(112, 118, 141, 232)*. The conductivity gradient was measured and taken into account in only five of the above-mentioned applications *(101, 103, 104, 214, 313)*. In three further studies it was measured and found to be negligible *(23, 66, 192)*. Three-dimensional CSDs have been derived from focally evoked potentials by Freeman (65), in a study of regeneration in the toad optic tectum, and by Hoeltzell and Dykes (112), in a recent study of cat somatosensory cortex.

Technically the most elaborate CSD analyses were carried out by Nicholson and Llinás (220), by Nicholson et al. (217), and by Breckow et al. *(23)*. Using clusters of seven microelectrodes fixed together so the tips were arranged equidistant in a three-dimensional grid, they performed real-time, three-dimensional CSD analyses. Nicholson et al. *(217)* even combined this method with the determination of the extracellular [K^+] by using an ion-selective electrode as the central pole. The experimental difficulties in building these elaborate multielectrodes, the expensive electronics for the on-line signal processing, and the increase in tissue damage and distortion due to the complex electrode arrays, however, will probably prevent this type of application from becoming a common tool.

Simultaneous recordings of one-dimensional potential profiles, on the other hand, have been performed in several recent CSD studies *(231, 251, 252, 314)*. Either thin-film metal electrodes *(150, 234, 240)* or multiarrays with equidistant tips constructed from isolated wires *(134, 183, 211)* or from micropipettes *(194)* were used. This type of simultaneous recording with a multielectrode has great advantages. It saves time and hence permits the recording and comparison of many different types of potentials within a period of time, during which the state of the animal as well as the positions of the electrodes in the tissue can be assumed constant *(194)*. It can be applied to record field potentials in freely behaving animals *(134, 143, 177, 183, 201)*. Furthermore, it gives access to unique events. Tissue damage and distortion are also a central problem with the available one-dimensional arrays, however.

A few studies, where the current flow density was extracted from the potential profiles by applying *Equation* 4 instead of *Equation* 5, are closely related to CSD analyses (e.g., refs. *152–154, 305, 306)*. With this type of

analysis, far fields are also eliminated, but the advantage of localization is utilized only partially. Because the extracellular current flow is secondary to the physiologically most relevant sinks and sources, this method does not have any advantage over the CSD method.

C. Interpretation of CSDs

The ambiguity of field potentials and CSDs with respect to the neuronal activities that cause them can only be overcome with additional information (see Fig. 1). The core-conductor theory supplies the relation between membrane currents and neuronal activities. Anatomical and single-unit data from the specific ensemble under investigation can help track down the summation of these currents from individual elements to the macroscopic sinks and sources (***Eq.*** 1). Furthermore, direct experimental manipulations, like repetitive stimulation or application of pharmacological agents, may give the cues to differentiate the types of the contributing neuronal activities. The basic arguments along these lines are summarized in this section (see also ref. 172).

1. Implications of core-conductor theory

The theoretical basis for the relation between membrane currents and neuronal activities of individual elements is well established in the core-conductor theory (110, 246)

a) Activation of axons and axon terminals. Activations of axons cause triphasic membrane currents, inwardly directed at the central site of activation and outwardly directed in front of and behind this zone (178). Due to the rather standardized duration of APs of ~1 ms, the spatial extent of this triphasic membrane current along the axon is proportional to the conduction velocity of the fiber. A conduction velocity of 20 m/s, for example, implies that the instantaneous membrane current is distributed over 20 mm! In the end-arborizations of an axon, the conduction velocity of the AP is markedly reduced, because these branches are nonmyelinated and smaller in diameter (57, 84). Generally it is assumed that the active spike does not invade the presynaptic terminals in the central nervous system (CNS) (97); they are depolarized by the capacitive outward current that flows in front of the AP.

b) *Synaptic activation.* During excitatory synaptic activation, active ionic current flows into the cell at the site of the synapse, and passive (capacitive and ohmic) current of equal amplitude leaves the cell at proximal and more-distant membrane sites (49). Both of these membrane currents are purely monophasic. The spatial distribution of the passive outward current over the cell membrane is determined by the length and the time constant of the cell membrane and by the time function of the active current (246). It decays exponentially, and its time function dissipates with the distance from the synaptic site. Quantitative estimates were obtained by model calculations: within 0.5–1 length constant, the amplitude of the passive outward current is reduced to 10–30%, its time function is dissipated by a factor of ~2, and the amplitude peak is delayed by ~0.5–2 ms (9, 123, 125, 173, 244). [Length constants in the range of 0.5–1 times the length of dendrites (124, 131, 212) and time constants in the range of 4–24 ms (124,131,182) have been reported.]

The excitatory postsynaptic potential (EPSP) is caused by the charging of the membrane capacitors by the capacitive outward currents. Therefore the amplitude of this current at any location is proportional to the time derivative, i.e., to the slope of the local PSP (8, 244). The return of the intracellular potential from the PSP peak to equilibrium essentially results from the discharging of the membrane capacitors via the local membrane resistors; therefore, no net membrane current flows during this decay phase. During hyperpolarizing inhibitory synaptic activation, the directions of the active and passive currents and of the PSP are reversed; otherwise, in principle, the situation is identical.

However, the locations of the two types of synapses on the neurons commonly differ. Most inhibitory synapses are located at or very proximal to the somata; the excitatory synapses spare the somatic membranes and occupy proximal and distant dendritic sites (31, 32, 59, 93, 236, 242, 254, 256, 285,296,301). The dendritic location of the excitatory synapses suggests that the amplitudes and time functions of the active synaptic inward currents at the dendritic sites cannot be judged from the somatically recorded EPSPs, which are due to the small fraction of the total capacitive current that leaves the cell at the soma membrane. The active inward currents at the dendritic synaptic sites are more coherent and are, on the average, 5–20 times larger than a direct estimate from the slopes of the somatic EPSPs suggest (9, 125, 173, 244).

The strategically optimal location of the somatic inhibitory synapses has different implications. According to geometrical considerations, a large portion of the capacitive current leaves the cell directly through the soma membrane, thereby causing the inhibitory PSP (IPSP). Therefore the time course and amplitude of the active outward current at the synaptic site are well reflected by the slope of the IPSP. The net somatic membrane current results from the difference between the active ionic outward current and the somatic (capacitive and ohmic) inward current. This net somatic outward current is the counterpart of the dendritic membrane currents that flow during this inhibitory synaptic activation. In the nomenclature used by Rall (244), the current flowing into the dendrites is the loss current from the soma compartment. A quantitative estimate of this loss current can be obtained from the phase-frequency diagrams, calculated by Lux (181), for different values of the ratio of dendritic input conductance (ρ) (245). Assuming $\rho = 3$

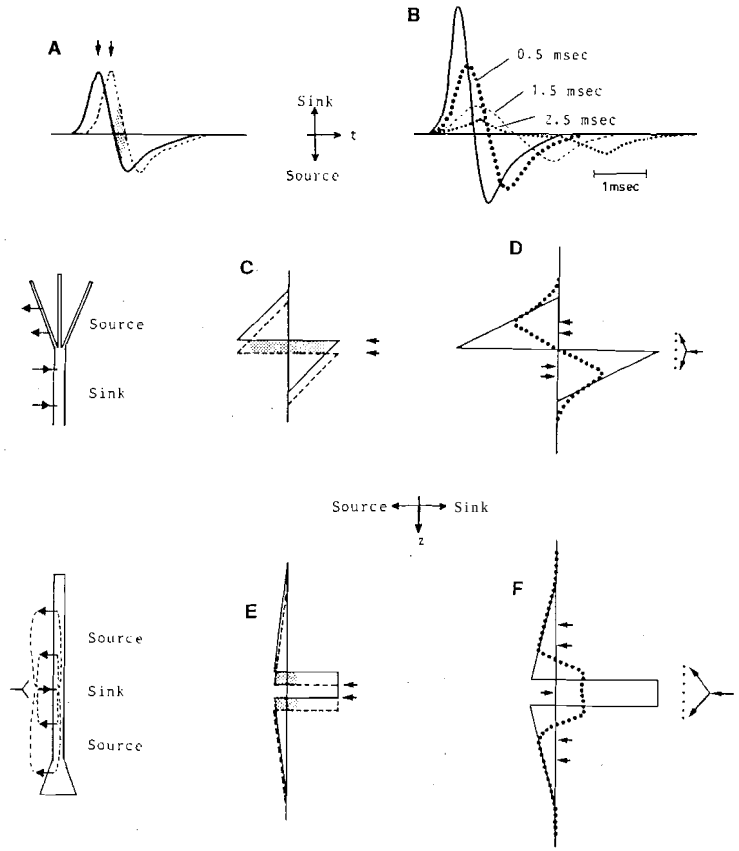

FIG. 2. Schematic illustration of cancelling effects of membrane currents in extracellular space due to temporal and spatial scatter of events. *A:* each *curve* represents time function of net somatic membrane current that flows during generation of soma action potential (AP). Amount of membrane current cancelled in extracellular space due to latency difference of 0.25 ms between the 2 APs is indicated by shaded area. [Curve adapted from Fig. 3a of Terzuolo and Araki (303).] *B*: solid *line* represents time function of current source density (CSD) at soma level of cell ensemble, caused by coherently evoked APs (identical to time function in A). Change of this CSD time function on temporal dissipation of APs is illustrated for scatter of 0.5 ms (*large* dots), 1.5 ms (dashes), and 2.5 ms (small dots). At scatter of 2.5 ms, a CSD-free zone appears between sink and source. *C*: each curve represents spatial distribution of CSD (at some time) along group of accurately aligned activated fiber terminals, as indicated in inset on *left*. (Exponential decays have been approxiniated by linear decays.) Because of steep transition between sink and source, small differences in depth have large cancelling effects (shaded area). *D*: CSD caused by activation of accurately aligned fiber terminals (solid *curve*) becomes smaller in amplitude and smoothed at sink/source transition zone, if terminals scatter in depth (dotted *curve*). Distance between equivalent planes (arrows) of sink and source is enlarged due to scatter. *E*: each curve represents spatial distribution of CSD (at some time) along a group of accurately aligned cells, caused by excitatory synaptic activation, as indicated in inset on *left*. Due to scatter in depth of elements, cancelling occurs at sink/source transition zones (shaded areas). *F*: CSD caused by excitatory synaptic activation (or by first phase of APs) of accurately aligned neurons (solid curve) becomes smaller in amplitude and smoothed at sink/source transition zones, if elements scatter in depth (dotted curve). Distances between equivalent planes (arrows) of sink and sources become larger.

(131, 212), the dendritic loss current is 75% of the active somatic current in the steady-state condition; at active current frequencies of 10, and 50 Hz and 1 kHz, this portion is reduced to 56, 47, and 11%, respectively.

c) Somatic and dendritic APs. During the generation of APs in nerve cells, as in fibers, the current flow is triphasic. At the same membrane location, the passive depolarizing outward current is first followed by inward current and then by outward current; the latter two are the net results of active sodium and potassium currents and a local capacitive current (110). In most cell types the AP is generated in and restricted to the cell soma (e.g., ref. 174).

In the hippocampal pyramidal cells (323), the cerebellar Purkinje cells (174, 219), and immature neocortical cells (243), however, specific types of APs may already be generated in the apical dendrite and may propagate actively down to the soma. These dendritic APs have much slower time courses (3–10 ms in duration) than the usual somatic or fiber APs; their conduction velocity is —0.2 m/s (219). The spatial distribution of membrane currents during the propagation of an AP along a dendrite is similar to that occurring during the propagation of a fiber AP. Capacitive outward current flows in front, and inward and outward currents follow. Probably due to the different types of membrane mechanisms involved here (42, 175), the spatial extent of these membrane currents along the dendrite is smaller (219).

The spatial and temporal distribution of passive as well as active membrane currents during the usual type of somatic AP is rather complicated. The active current can be assumed to be restricted to the soma membrane. The dominant frequency component of this active biphasic current is —1 kHz. Therefore, only 11% of this current is loss current that flows through the dendrites (see above); 89% of it is compensated at the soma membrane, essentially by capacitive current. Because the loss current is identical to the net somatic membrane current, its time course can be estimated from the extracellular potential generated at the soma membrane during the AP (303). A typical example of such a time function is shown in Figure 2*A*. It is biphasic, and its dominant frequency component is —1 kHz. Due to this high temporal frequency, the amplitudes of the passive dendritic membrane currents decay much more steeply with the distance from the soma than those

flowing during the slower inhibitory events (123). This implies that most of the passive current flows proximal to the active current; therefore the corresponding extracellular current loops are confined to the close vicinity of the soma. This is reflected by the empirical fact that the amplitudes of extracellularly recorded APs decay rapidly on retraction of the electrode from the soma (19, 206, 303).

d) Glial cells. The contribution of glial cells to extracellular potentials has been dealt with in several reviews (e.g., refs. 30, 52, 226, 241). The neuroglia appears to be the main cause of slow potentials with frequencies < 1 Hz. In the CNS, significant contributions to faster events can be ruled out according to intracellular data from the cat cortex: the electrically evoked or spontaneous potential changes in these glial cells occur much later and are slower and smaller by a factor of 10 than corresponding PSPs in neurons (95, 96, 249, 250). This implies that the membrane currents of neuroglia are smaller by a factor of 100 and are negligible in comparison with membrane currents from neuronal activities.

In the retina the situation appears to be different. Here the Miiller cells are the only elongated processes, which are oriented perpendicularly to the neuronal and plexiform layers. These glial cells have peculiar conductance properties (214a). Their intracellular potentials correspond well with the b-wave of the electroretinogram, which has a rise time of —200 ms (191). It has therefore been suggested on the basis of a CSD study that the b-wave is caused by K+-currentflow into the Müller cells within the plexiform layers and corresponding outflow at the extreme distal end of the retina (214, 215).

2. *Summation of membrane currents to macroscopic sinks and sources*

To understand the transition from the microlevel of the membrane currents to the macrolevel of the sinks and sources (*Eq.* l), each type of mass activation is considered in an idealized arrangement, then the realistic deviations from this model are outlined.

The idealized arrangement consists of identical elements that are precisely aligned in a two-dimensional sheet; one type of activation is assumed to occur identically and synchronously in all elements In these cases the extracellular volume average of the membrane currents (Eq. 1) can be concluded directly from the individual membrane currents, and the simplest possible CSD distributions result. Because these are homogeneous in the two directions parallel-to the sheet, only the direction perpendicular to the sheet is of concern.

a) Activation of axons and axon terminals. Activation of fibers results in a source/sink/source distribution. This source/sink/source sequence passes through the sheet at the conduction velocity of the fibers. Even for the slowest types of fibers, it extends over 1–2 mm. This implies that the amplitudes of the sink and the two sources are low, compared with more localized events Furthermore, this dissipated CSD distribution is not resolvable in the usual type of CSD applications designed to study a cortex or a nucleus and optimized to resolve events that extend over —50–300 μm (Eq. *8).*

In contrast to the activation of fibers of passage, the activation of terminal arborizations results in a localized sink/source distribution (196, 197). The sink probably results from the last active inward current, and the source in front of it is due to the leading capacitive outward current. This interpretation agrees with the shapes of potentials in the vicinity of cut nerve endings, as described by Lorente de Nó (178). However, because the main components of the afferent activation — the preceding dissipated sinks and sources — are not resolved, this interpretation must remain tentative.

A slight scatter in depth of the terminals leads to a corresponding expansion of the sink and source depth regions. At the external borders, the amplitudes of the sink and source decay according to this scatter. At the central sink/source transition zone, however, nearly total cancellation of opposite membrane currents from nonaligned elements occurs in this situation (Fig. 2*C*). Due to this central cancellation, the distance between the equivalent planes of the resulting sink and source is increased (Fig. 2*D*). Temporal dissipation of the afferent impulses leads to a prolongation and a proportional amplitude reduction of the CSD. This temporal scatter does not cause any cancellation, because the time course of the CSD is monophasic. Examples of this type of activation are the primary afferent activities of the neocortex (197) and of the lateral geniculate nucleus (LGN) (196).

If the fibers (e.g., the cerebellar parallel fibers, the primary afferents of the optic tectum) enter a nucleus tangentially and terminate throughout this layer, the terminals are evenly scattered. In this situation the membrane currents of the terminal regions cancel totally. Therefore, the sink recorded in experiments in such layers of terminals (65, 67, 313) must be due to excess inflow of current into the fibers that terminate at the far end; i.e., in this situation, more of the central sink of the dissipated source/sink/source distribution reaches the nucleus; the counterpart of the resulting excess sink, the final source, does not enter the nucleus.

b) Synaptic activation. Synchronized excitatory (inhibitory) synaptic activation of a sheet of neurons creates a sink (source) at the depth of the synapses and creates sources (sinks) above and below the synapses. Because these sources (sinks) do not extend beyond the neurons, synaptic activation at the far upper or lower ends of the neurons creates a dipolar sink/source distribution only. Because the amplitudes of the passive capacitive currents decay exponentially with the distance from the synápses, the amplitudes of the sources (sinks) decay exponentially with the distance from that synapse level as well. The time functions of these sources (sinks) are more coherent than the time function of the central sink (source) and peak slightly earlier, close to the synaptic level; with distance, they progressively dissipate and peak later. Obliquely arranged dendrites imply a compression of the source (sink) distribution and thereby a reduction of the distance of the equivalent

source (sink) plane from the synaptic plane, but no quantitative loss. The only exception is the horizontal dendrites within the synaptic plane; the source, due to their passive currents, subtracts from the sink.

The effects of scatter of the synaptic activations in depth or time are very similar to those described above for terminal arborizations. Because of the scatter in depth, cancellation occurs at the sink/source transition zones (Fig. 2*E*), thereby smoothing the steep sink/source gradients and increasing the equivalent plane distances (Fig. 2*F*). The spatial expansion at the outer borders of the CSD and the temporal dissipation cause proportional amplitude reductions but no cancellations.

c) Somatic and dendritic *APs.* Synchronous generation of APs in the somata of accurately aligned cells creates a sink, succeeded by a source, at the depth of the somata (see Fig. 2*A*), and a source, then sink, above and below the somata. The amplitudes of the distributions of source followed by sink decay steeply with the distance from the soma region. Obliquely or horizontally oriented dendrites have the same implications here as they do for the passive sources (sinks) during synaptic activations.

Qualitatively, scatter of the somata in depth has the same effect as scatter of synapses, with cancellations at the sink/source transition zones and dissipation of the CSD distribution (see Fig. 2*E*, **F**). Quantitatively, however, this effect is more severe here, because the distances of the equivalent sink and source planes are much smaller (123); i.e., a small amount of scatter in depth of AP-generating somata is equivalent to a much larger scatter of synapses, with respect to the cancelling effect. In contrast to the situation during terminal or synaptic activations, temporal scatter of the APs also causes cancellations, which are due to the biphasic nature of the CSD time function (see Fig. 2*A*). The change in the time function and the amplitude reduction of the CSD due to temporal scatter of the APs is illustrated in Figure 2B. Because of the smooth transition between the sink and the source, the effect of cancelling is rather small for small scatters (see Fig. 2A). It steadily increases up to a scatter of —1.5 ms. From then on, the sink and the source (and their corresponding counterparts above and below) do not dissipate any more. Further scattering leads to a further amplitude reduction and an increasing CSD-free zone between (see Fig. 2*B*). Now all the membrane currents from the successive APs cancel totally; only the first phase of the earliest APs and the last phase of the very last APs remain imbalanced.

The dendritic APs in the apical dendrites of Purkinje cells and hippocampal pyramidal cells cause a source/sink/source distribution, which moves down to the soma level at a velocity of —0.2 m/s. Its instantaneous extent over depth is —300 μm (219). Its triphasic time function — according to the slow time course of the dendritic APs — has a duration of at least 3 ms. The smooth transitions between the sink and the sources, in space as well as in time, imply that small scatter in latency (and the concomitant spatial scatter) have only slight cancelling effects (see Fig. 2*A*). In comparison to the soma APs (see Fig. 2*B*), the time range of scatter may be at least twice as long to cause equivalent effects.

3. Quantitative *comparison of AP- and* PSP-related CSDs *and* experimental *confirmations*

a) Theoretical *estimate.* By combining the considerations of the two preceding sections, a quantitative estimate of the CSD contributions from APs and PSPs can be made. Such a general estimate must be very rough, however, because of the uncertainty in evaluating the relevant parameters. The parameters considered for the present comparative estimate, and their assumed values, are listed in Table 1. Two sets of values have been selected to simulate coherent mass actions (e.g., activity evoked by electrical stimulation or related to coherent interictal spikes) and more dissipated mass actions (e.g., activity evoked by adequate natural stimuli or spontaneous rhythmic activity). The range of likely values was considered for the rise time of dendritic APs and for the fraction of loss current of dendritic EPSPs; in addition, values for very low scatter of APs are given. An equal density of neuronal elements and fibers was assumed. Activations of fiber terminals were not included in this estimate because the details of this process are not known well enough to make the appropriate assumptions (see sect. II*C2a*). The results for fiber APs, dendritic APs, soma APs, EPSPs, and IPSPs are given in the bottom two lines of Table 1.

According to this theoretical estimate, EPSPs cause the largest CSD amplitudes. Their dominance is mainly due to the factor that accounts for the dendritic location of the synapses. Even if the smallest of the corresponding values from the literature is chosen, the EPSPs still cause two to three times larger CSDs than APs in fibers or cell somata. The APs, although having much higher amplitude, are less effective, either because they are very dissipated (fiber APs) or because the fraction of the loss current from the soma is very small (soma APs). During natural activation, soma APs are totally negligible in comparison with EPSPs. This is because of the large cancelling effect, implicit in the biphasic nature of the time function, anti because of the small transfer ratio that must be assumed in this situation. The IPSPs are an order of magnitude less effective than APs or EPSPs. The insignificance of their contribution to CSDs essentially reflects the shallow $\partial V/\partial t$ gradients in comparison with APs and the EPSPs at their dendritic site of generation.

b) Fiber *APs.* The APs in fibers cause larger CSDs than soma APs. Because of their spatial dissipation, however, these CSDs are assessed experimentally only in special cases (see II*C2a*). Fibers larger in diameter and faster in conductance than those considered for the present estimate cause even larger CSDs; however, they are also more dissipated.

TABLE 1. Quantitative estimates of contributions of various types of neuronal activities to current source densities

	Fiber APs		Dendritic APs		Soma APs		EPSPs		IPSPs	
	Coherent	Dissipated	Coherent	Dissipated	Coherent	Dissipated	Fast	Slow	Fast	Slow
Amplitude ΔV (mV)	100	100	100	100	100	100	5[a]	5[a]	5[a]	5[a]
Time to peak ΔT (ms)	0.5	0.5	1.5-5	1.5-5	0.5	0.5	1	10[a]	3	30[a]
Relevant membrane area F (10^{-4} cm^2)[b]	0.09[c]	0.09[c]	0.16[c]	0.16[c]	0.28[d]	0.28[d]	0.28[d]	0.28[d]	0.28[d]	0.28[d]
Loss current/capacitive current = I_{max}/I_c	1.0[e]	1.0[e]	1.0[e]	1.0[e]	0.12[f]	0.12[d]	10[g] (5-20)	10[g] (5-20)	0.7	1.0[f]
Temporal scatter ΔT (ms)	1	10	1	10	1 (0.3)[h]	10	1 (0.3)[h]	10	3	30
Amplitude factor due to $\Delta T = a'$	0.3	0.03	0.7-1.0	0.1-0.3	0.3 (0.8)[h]	0.03	0.5 (0.8)[h]	0.5	0.5	0.5
Spatial scatter Δz (μm)	ND	ND	ND	ND	100	100	100	100	100	100
Amplitude factor due to $\Delta z = b'$	0.1[k]	0.1[k]	0.33[k]	0.33[k]	0.26	0.26	0.26	0.35	0.32	0.36
Transfer ratio = c[l]	1	1	0.7	0.3	0.7	0.3	1	1	1	1
Relative CSD amplitude $= \frac{\Delta V}{\Delta t} \cdot$ area $\mathbf{F} \cdot \frac{I_{max}}{I_c} \cdot a \cdot b \cdot c$										
Averages	0.54	0.05	1.23	0.11	0.36 (0.96)[h]	0.02	1.82 (2.91)[h]	0.25	0.05	0.01
Ranges	ND	ND	0.74-1.72	0.10-0.11	ND	ND	0.91-3.60	0.12-0.49	ND	ND

Parameters were seldcted to simulate electrical (coherent) and natural (dissipated) activation of an ensemble. APs, action potentials; EPSPs, excitatory postsynaptic potentials; IPSPs, inhibitory postsynaptic potentials; CSD, current source density; ND, no data. [a]See refs. 37, 41, 56, 210,318. [b]Relevant membrane area F is defined by $\mathbf{I}_m = c_m \mathbf{d}V/dt$, where maximum capacity $c_m = 2\ \mu$F/cm^2. [c]For fiber conducting at 1 m/s, 1 μm diam and 300 μm length of instantaneously depolarized segment were assumed. For apical dendrites, 5 pm diam and 100 μm length of instantaneously depolarized segment were assumed (219). [d]Because AP and PSP values are from soma, soma surface is relevant area; soma of 30 μm diam was assumed. [e]See ref. 110. [f]See text. [g]Dendritic location of excitatory synapses is considered (see text). [h]Scatter of only 0.3 ms may be appropriate in some cases of antidromic or strong monosynaptic activation via homogeneous, fast-conducting axons (e.g., refs. 56, 294). [i]See Figure 2*E* and text. [j]Reference value of 30 μm is assumed as depth extent of synaptic region and AP-generating membrane. For soma APs and fast EPSPs a factor of 0.26 was assumed, according to Figure 2*F*. Progressively higher values were assumed for slower PSPs, according to frequency dependence of spatial distribution of passive membrane currents (123). Values are proportional to distances of equivalent neighboring sink/source planes. [k]Spatial dissipation of APs along fibers or apical dendrites is considered; see footnote c. [l]Transfer ratio equals number of APs per stimulus (e.g., refs. 75, 79, 109, 294).

c) Dendritic APs. Dendritic APs cause CSDs comparable in amplitude to the CSDs evoked by excitatory synaptic activations. This theoretical result is in good agreement with experiments. In the hippocampus, where dendritic APs are presumed to occur predominantly (323), the field potentials contain a "population spike" with an amplitude in the same range as the amplitude of the EPSP-related component (7). CSDs from hippocampal slices, evoked by suprathreshold stimulation of the stratum radiatum afferents, consistently show a sink (and corresponding sources above and below) in the depth region of the apical dendrites and the somata of the CA1 neurons. The latency of this sink increases toward the soma at ~0.5 ms/100 μm. The amplitude of this sink is about equal to the amplitude of the sink caused by the synaptic activation (272; W. Zieglgänsberger and U. Mitzdorf, unpublished observations). In the alligator cerebellum, Nicholson and Llinás (219) demonstrated a contribution of dendritic APs to field potentials. There too the amplitudes of the contributions from the dendritic APs and from the synaptic activation are similar. Dendritic APs have also been identified, or proposed, as significant contributors to CSDs in several further studies (153, 161, 295, 313).

d) Inhibitory synaptic activations. According to the present estimate, IPSPs do not contribute significantly to CSDs. Indeed, in most CSD studies of synaptic organizations, no contributions attributable to IPSPs were found in the optic tectum (28, 67, 295, 313), the cerebellum (68, 153), the visual cortex (197, 198), or the hippocampus (102). Minor contributions from IPSPs were identified, or assumed, in studies in the prepyriform cortex (101), the LGN (196), the hippocampus (161), the cerebellum (66, 154), and the neocortex (306). A model calculation of evoked potentials, based on single-unit data from the cat somatosensory cortex (305), yielded a proportion of 5:1 for EPSP- versus IPSP-related components.

Correlations of major CSDs with IPSPs were found in two CSD studies (3, 122). The large-amplitude CSD, which Humphrey (122, 123) definitely attributed to IPSPs, actually does not contradict the present estimate, because it can only be elicited by extremely unnatural stimulation (antidromic train stimulation of the pyramidal tract). The large late CSD evoked in the dentate gyrus by stimulation of the perforant path (3) may be an exceptional example for a significant contribution from inhibitory synaptic activation (at the somata). Quantitatively, however, the contribution of IPSPs to the late CSD could not be assessed in that study, because it could not be segregated from contributions evoked by the late phase of the excitatory synaptic activation and the postspike repolarization (4). IPSPs have definitely been identified as the predominant causes of two pathological spontaneous phenomena [the wave of the spike-wave complex (235, 237), the surface-negative type of the delta wave (268)] and of the second surface-negative wave, which sometimes follows the direct cortical response (DCR) (237).

e) Soma APs. According to the present estimate, soma APs can be ignored totally, if temporally dissipated mass actions are investigated. This result is in agreement with all the earlier correlative studies of EEG waves and

single units (for reviews see refs. 35, 241, 270). Even during coherent activations, however, AP CSDs are still about five times smaller than the EPSP CSDs. Only if the scatter of the APs is very low may their contribution become about equally significant (see Table 1). Eccles (48), in accordance with this result, reviewed electrically evoked potential data from cerebral cortex and reached the conclusion that EPSPs were the most probable causes of all these potentials. Since then, further affirmative data have been obtained. In CSD studies of the LGN and the visual cortex, it was demonstrated that the contributions of APs are usually small, compared with the contributions of synaptic activations (196–198). Among these thalamic and cortical relay stations, the monosynaptic activation of cat area 18 should be the component where APs contribute most, because the latency scatter is very low (0.4 ms; 213, 294, 307, 308), and the involved synapses are located on proximal dendrites (197). To make a quantitative estimate for this activation, single unit-data are available. On double-shock stimulation of the primary afferents, the sink of the second response is reduced by 30% (197; U. Mitzdorf, unpublished results), and the number of corresponding APs is reduced by 56% (G. Neumann, personal communication), which implies a contribution of 54% from the APs. This result from experimental data agrees rather well with the corresponding theoretical value for APs, compared with EPSPs from proximal synapses (0.9:1.4). [According to other experimental results, however, this estimate appears to be too high (see sect. III*A2*).]

Nicholson and Llinás (219) indirectly demonstrate that orthodromically evoked soma APs contribute little to the field potentials. Their model calculation of synaptic activation fits the experimental data from the cerebellum very well, although they did not consider APs in their model. Towe (305) could best fit his evoked-potential data from the cat somatosensory cortex by considering PSPs, not APs, in his model calculations. Furthermore, no component is attributed to soma APs in any CSD study of electrically evoked potentials published to date.

The correlations found in many studies, between single-unit responses and peaks of the evoked potentials (e.g., refs. 71, 99, 253, 320), do not contradict the assumption that EPSPs, not APs, are the main causes of the evoked potentials. Because EPSPs cause the APs, such a correlation is to be expected (see also ref. 63). Also, the studies where the responding cells were found in the same cortical depths as the sinks (314) or the negativities of the field potentials (115) may still be interpreted by the causal relationship between EPSPs and APs. According to the depth of the sinks and the potential negativities in both studies, the activities in question were monosynaptic intracortical activities. Because the afferents mainly contact small stellate cells and pyramidal cells at their proximal dendrites (197), this depth correlation of the monosynaptic activity and the APs is very likely.

Antidromically evoked APs, which occur in most of the deep pyramidal cells of the cat visual cortex after stimulation of the optic radiation, have a latency scatter of ~6 ms (86,106,279,308). In agreement with the theoretical considerations, no contribution of these scattered APs to CSDs was found (197). A CSD component resulting from the antidromic activation of pyramidal tract cells was identified by Humphrey (122, 123). Its amplitude was ~40% of the CSD, which was evoked concomitantly by recurrent excitatory synaptic activation. If the latency scatters (1.5 ms for APs, 6 ms for EPSPs) and the distribution of the cell somata over cortical depth (see ref. 123) are taken into account, a theoretical estimate of the relative sizes of the two contributions agrees well with the experimental results. Antidromic activation of Purkinje cells results in a contribution to the field potential (219) or the CSD (66), which is slightly larger than the concomitantly evoked synaptic activation. Because the latencies of these APs show little scatter, and because the somata of the Purkinje cells are rather precisely aligned, these results conform with the theoretical estimates of Table 1 as well.

f) Summary. The theoretical estimate of the relative contributions from APs, EPSPs, and IPSPs to CSDs (Table 1) is justified by its agreement with many experimental results. It leads to the conclusion that EPSPs are essentially the dominant causes of the CSDs. Correspondingly, most experimental CSD studies were designed to yield information about excitatory synaptic ensemble activities. Most of these studies focused on finding out or confirming physiologically where the afferents terminate in the nucleus or cortex under investigation (23, 28, 64, 65, 102, 141, 153, 154, 186a, 196). In several others the polysynaptic organization of excitatory circuits was investigated with the CSD method (101, 197, 198, 313). The method was also applied to assess effects of deprivation, regeneration, conditioning stimulation, or drugs on excitatory synaptic mass actions (65, 67, 140a, 195, 200, 277, 278, 306).

4. Distinction between *CSD contributions* from *different* types of *neuronal* activity

Although EPSPs are the dominant causes of CSDs, significant contributions from presynaptic activity, APs, or IPSPs may occur. They cannot be ruled out from the onset when studying the mass actions of a nucleus or cortex with the CSD method. Cues for a distinction of the contributions from these different types of activity may come from any field of neuroscience. Here the principal relevant arguments are briefly reviewed.

The most direct help comes from anatomical and single-unit studies about the ensemble under investigation. Data from extra- and intracellular single-unit recordings help to identify CSD components by the argument of temporal coincidence; the latency scatter of individual events helps to estimate the likelihood of summation of the related membrane currents (101,102,123, 140a, 186a, 196, 197, 312). The most important anatomical aspects are the types and degrees of orderliness within the ensemble. Anatomical data may disentangle the ensemble into subgroups of similar elements. The geometries

of these elements, their density, and the degree of their alignment and spatial scatter are essential cues. They help to attribute CSD components according to spatial correlations, according to the succession of events as determined by the circuits, and according to quantitative arguments about summation properties of elements (101, 102, 123, 153, 154, 196–198, 235, 272, 295, 313).

In addition to these sources of information from separate anatomical and physiological studies, essential cues may be obtained by varying the mass actions of the ensemble. Stimulation of the afferents at different locations along their path helps to disentangle the contributions due to fast- and slow-conducting afferents, according to the differential latency changes of the CSD components (196–198, 312, 313). According to their different thresholds, fast- and slow-conducting fibers may further be differentiated by variation of the stimulus strength (141, 312, 313). Train stimuli or double stimuli may help to distinguish between pre- and postsynaptic components, or between mono- and polysynaptic components, according to the differences in their recovery cycles (3, 28, 101, 118, 196–198, 272, 312, 313). Local or systemic application of pharmacological agents, which either attenuate or facilitate specific mechanisms, can help to a'ttribute CSD components according to their amplitude changes caused by the drug (3, 28, 65, 67). [The practices of repetitive stimulation and drug application were already common tools in the pioneering studies of evoked potentials (e.g., refs. 10, 11, 18, 43, 60, 186).]

III. CURRENT SOURCE-DENSITY ANALYSIS OF EVOKED POTENTIALS IN CAT VISUAL CORTEX

This description of an experimental application illustrates the theoretical arguments given above. In two series of studies (193, 194, 197, 200), field potentials evoked by electrical and visual stimuli were recorded in primary visual areas 17 and 18 of the cat cortex (acute experiments; anesthesia: pentobarbital and/or N_2O) and were subsequently subjected to CSD analysis. The use of different types of stimuli and comparisons with anatomical and single-unit data helped to interpret the CSDs. With the wealth of known anatomical and physiological facts about the cat visual cortex, it was possible to identify the origins of the sinks and sources. Their spatiotemporal distributions revealed new aspects of the intracortical processing of afferent information. The main arguments and conclusions of these experimental studies are outlined in this section.

A. Electrically Evoked CSDs

Most of the electrically evoked field potentials were recorded with one micropipette, which was successively placed at different cortical depths. The recordings were made equidistantly at $\Delta z = 50$ or 100 pm. From these profiles, the one-dimensional CSDs were calculated with a differentiation grid of $n \cdot \Delta z = 200\ \mu m$ (see *Eq. 8*), while the intracortical conductivity was assumed constant (see sect. II*A*). An example of such a potential profile and the corresponding CSD profile is given in Figure 3*A*, B.

1. *Relation* between potentials and CSDs

A cursory comparison of the two profiles in Figure 3 already demonstrates the localizing effect of the CSD method. Whereas the various peaks of the field-potential profile are widely dissipated over depth and have large amplitudes even in the white matter below the cortex, the CSD profile is well structured and reveals discrete events. In the potential profiles, some of these local events are totally hidden among large-amplitude far-field components (e.g., component f in Fig. 3B: the large sink and the corresponding sources above and below create a closed-field component, which is barely recognizable in the potential profile).

In area 18, electrical stimulation of the primary afferents evokes a potential that is roughly mirror symmetrical at the surface and in the white matter (see ref. 197). Therefore the generators of this potential are located between these two depths (see sect. II*A*). In area 17, on the other hand, the surface potential is very small, whereas the white matter potential has large-amplitude peaks (see Fig. 3*A*). The asymmetry indicates that large far-field components contribute to this potential. These probably originate in other regions of area 17. This area occupies roughly a hemisphere at the occipital pole and is evenly activated by stimulation of the primary afferents. The occipital pole, viewed as a whole therefore generates a "closed field" (140), with a large-amplitude potential at the center of the sphere (i.e., in the white matter) and only minor deflections at the surface (i.e., at the cortical surface).

Because the surface potential over area 17 is the rather arbitrary and small result of the superposition of the large locally generated component and the large (inverted) far-field component from "opposite" regions of area 17, it does not contain any useful information. The peaks of the surface potential over area 18, on the other hand, can be attributed to underlying local events (197). This surface potential, which is essentially caused by activity within area 18, has erroneously been attributed to area 17 in earlier works (for review see ref. 36).

2. *Interpretation* of CSDs

To identify the neuronal activity causing the sink and source peaks within areas 17 and 18 (e.g., Fig. 3*B*), stimuli were applied in the optic radiation (OR), in the optic chiasm (OX), at the optic nerves (ON), and within the cortical areas themselves. These stimuli were presented as double shocks with a 20-ms interstimulus time, and their strength was varied. In addition,

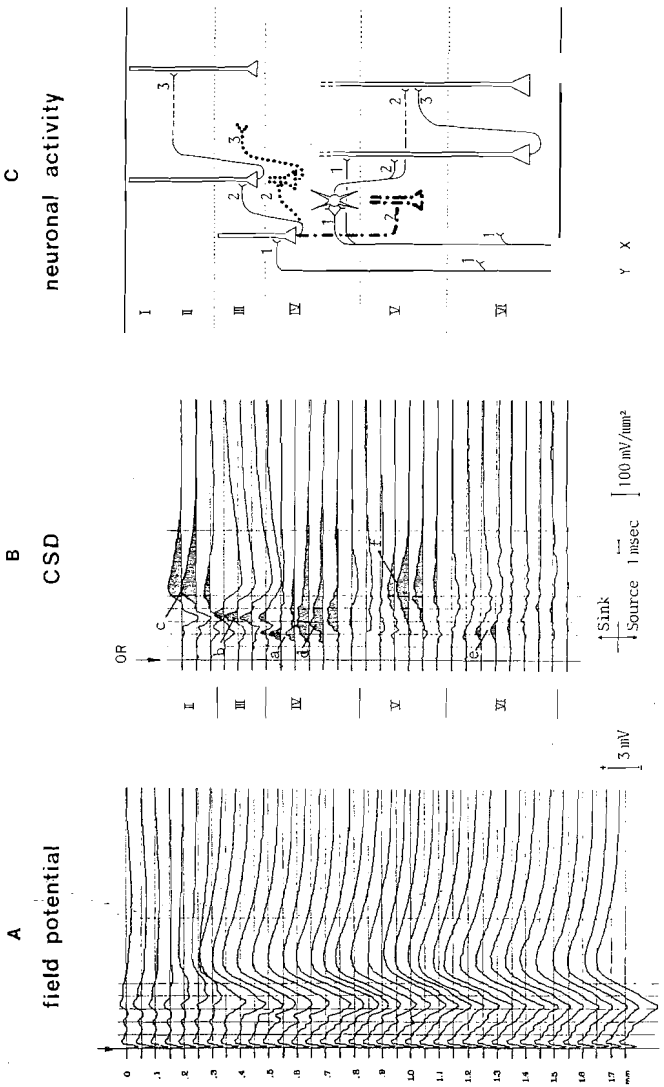

the effects of two pharmacological agents (picrotoxin and pentobarbital) were investigated.

Comparison of OR-, OX-, and ON-evoked CSDs in area 18 confirmed that this area is activated essentially by the fast-conducting Y-type afferents (264, 294, 308). On stimulation of the afferents at the farther sites, the CSD as a whole was delayed; however, it was not more dissipated. The CSDs in area 17, on the contrary, were more dissipated. According to their differential latency increases, the components could be attributed either to Y-type activity mediated by the fast-conducting afferents or to X-type activity mediated by the slower-conducting afferents. The earliest sinks and sources of each group could then be attributed to monosynaptic activity and all later components to polysynaptic activity mediated by intracortical connections.

The CSDs evoked by the second of the double shock in OR are consistent with this latter point; when the second afferent volley arrives in cortex, the cells are under strong inhibitory influence due to the first activation (213, 279, 307, 308). This inhibition does not affect the monosynaptic activation, but it prevents the generation of APs in many cells. Accordingly, the sinks and sources, which had been attributed to monosynaptic activation, were still present in these CSDs; those components that had been attributed to polysynaptic activation, however, were drastically reduced or totally missing. The attribution of two sink/source components to polysynaptic activities, according to the above arguments, could further be confirmed by intracortical stimulation. Direct stimulation of cortex several millimeters distant from the recording site evoked predominantly those polysynaptic components. In addition, this result implies that long-distance connections are involved in the mediation of these polysynaptic activations.

Picrotoxin and pentobarbital were applied systemically to investigate

FIG. 3. *A:* field potential in primary visual cortex (area 17) of cat evoked by electrical stimulation of optic radiation (*arrow*). Stimulus was preceded by stabilizing stirnulation of reticular formation (see ref. 197). Each *trace* is average of 20 responses. Distance between adjacent recordings is 50 pm. Profile was obtained by successive recordings with 1 micropipette. B: current source-density (CSD) distribution obtained from potential profile in A, according to Equation 8, with differentiation grid of $n \cdot \Delta z$ = 200 pm. According to *Equation* a', highest and lowest regions of recording range are missing in CSD profile. Sinks, corresponding to active excitatory postsynaptic potential currents, are shaded At *left*, depth regions of cortical laminae are indicated. Sinks a, b, and c reflect mono-, di-, and trisynaptic Y-type activity; sinks d and f reflect mono-, di-, and trisynaptic X-type activity; sink e reflects Y-type and X-type monosynaptic activity. *C*: schematic diagram of successive intracortical excitatory relay stations as well as cell types involved, as suggested by CSD in B and similar findings (see sect. IIIA). Three main pathways along which afferent activity is relayed within the visual cortex were revealed (long-distance connections are indicated by dashed lines; numbers indicate whether activations are mono-, di-, or trisynaptic). First pathway transmits afferent Y-type activity from upper layer IV to layer III and then to layer II. Second pathway relays afferent X-type activity from lower layer IV to layer V, where mainly lamina VI pyramidal cells are contacted (di- and trisynaptically). Along third pathway (dotted *connections*), Y-type afferent activity is relayed within layer IV and then projected to layer III. Y-type activation of lamina V cells, as suggested by single-unit studies, is also indicated (dash-dot connections).

whether inhibitory synaptic activity contributes to the intracortical CSDs. These drugs, respectively, are known to decrease (e.g., ref. 20, 78) or increase (e.g., ref. 222) the strength of inhibitory synaptic activation. After the application of picrotoxin, all the sinks and sources of the OR-evoked CSD were increased in amplitude. This effect was rather minor on the monosynaptic components and was large on the polysynaptic components; the latest polysynaptic components sometimes increased in amplitude up to a factor of 10. Pentobarbital had the opposite effect: monosynaptic components were only slightly reduced, polysynaptic components were strongly reduced or totally blocked. None of the sinks or sources was increased by pentobarbital. These results indicate that none of the CSD components were due to inhibitory synaptic activation. The small drug effects on the monosynaptic components (3-10%) further indicate that even the monosynaptic components mainly result from synaptic activity and only to a small extent from APs. Discrepancies in estimates of AP contributions (see sect. II*C3*) may either originate in the imponderable amounts of shunting effects (e.g., in the second CSD responses to double shock, due to simultaneously acting inhibition), or they could be due to a sampling bias in the single-unit data used for the estimate in section II*C3*.

Tonic and evoked inhibition in the cortex as well as in the thalamic relay stations were indirectly accessible, according to their effects on the excitatory activity. In area 18 the responses to the first of the OR double shocks were very consistent and reliably evoked, indicating that tonic inhibition has little effect on the intracortical transmission of primary afferent activity in this area; the evoked inhibition is not effective here, because it lags behind. In area 17, in contrast, the polysynaptic components were rather variable from one recording to the next. This variability indicates that inhibition is more effective in this area. In addition to tonic inhibition, evoked inhibition can also influence the intracortical transmission of primary afferent activity here, because the afferents mediating excitation in area 17 are slower conducting.

The fully developed evoked inhibition in the cortex was accessible in comparison between the polysynaptic components of the first and the second CSD responses to double-pulse stimulation in the OR; it is strong in both areas (see above). Comparison of the monosynaptic components in the first responses to OR stimulation with those to OX stimulation reveals filtering properties of the thalamic relay stations; whereas the afferent activity to area 18 is only mildly affected by the thalamic filter (−30%), both the Y-type and the X-type afferent activities to area 17 are drastically affected (−65%); i.e., many of the relay cells in the LGN projecting to area 17 do not reach the threshold level on afferent stimulation. The effect of the fully developed evoked inhibition in the thalamus could be seen by comparing the monosynaptic components in the first and second of the OX-evoked CSD responses; it usually blocked the afferent activity to area 17 nearly totally and blocked more than 65% of the afferent activity to area 18.

3. Information from CSDs

According to the above arguments, the CSDs are essentially caused by excitatory synaptic ensemble activity. Therefore the depths of the sinks indicate the laminar arrangements of the involved excitatory synapses; and the extent in depth of each sink and its corresponding source (or sources) indicates the depth region over which the activated cells extend their processes (see sect. II*C*). The successive intracortical excitatory relay stations, as well as the involved cell types suggested by the CSDs, are indicated in Figure 3*C* (see also ref. 197).

The monosynaptic sinks (a, d, and e in Fig. 3*B*) demonstrate that the afferent fibers terminate in laminae IV and VI. In lamina IV the Y-type afferents terminate above the X-type afferents. This result agrees with recent anatomical data (57, 88, 164). The Y-type afferents contact cells that extend into layer III. Likely candidates for this Y-type monosynaptic activation (sink a) are stellate cells in upper layer IV and pyramidal cells of lower layer III (179); they are symbolically indicated in Figure 3*C* by a pyramidal cell that extends over lamina III and upper lamina IV. Because a minor source was seen in layer V, some deep pyramidal cells may also be contacted by these fibers in layer IV. The X-type afferents mainly contact cells that do not extend into layer III; most likely candidates are stellate cells in layer IV (179); but because of a large source in layer V corresponding to sink d in lower layer IV, deep pyramidal cells are involved as well. Additional information about receptive-field properties and AP latencies of single cells (86, 228, 279) suggest that the deep pyramidal cells involved in the Y-type activation are lamina V cells, and those involved in the X-type activation are lamina VI cells.

The polysynaptic sinks demonstrate three main pathways along which the afferent activity is processed within the cortex. Along the first pathway (Fig. 3*B*, sinks a–c), afferent Y-type activity is projected to the supragranular layers. Lamina III pyramidal cells are activated disynaptically (sink b) at their proximal dendrites within lamina III via strong local connections. The same cell type is then activated trisynaptically (sink c) at the peripheral dendrites within layer II via local and long-distance connections. Along the second main pathway (sinks d and f), afferent activity is projected down to layer V. In area 17 the X-type afferent activity is relayed along this pathway. Because the long-lasting sink f in layer V draws much current from below, mainly lamina VI pyramidal cells are activated along this pathway. They are contacted within lamina V di- and trisynaptically via short and long-distance connections. The third pathway (not easily recognizable in the CSD of Fig. 3*B*) has one relay within layer IV, and then projects Y-type activity to lamina III (197). It is indicated in Figure 3*C* by dotted connections.

Thus the CSD study of visual cortex has revealed a further basic principle of topographic organization. The results demonstrate that the afferent and intrinsic excitatory connections are arranged in a lamina-specific manner.

The location of a cell with respect to the horizontal plane determines the retinotopic location, the ocular dominance, and the orientation preference of its receptive field (119, 120). The cell type and the laminar depth of its soma determines the destination of the cell output (87). According to the CSD results, the laminae in which the cell receives its inputs determine the type of input (Y type or X type; mono-, di-, or trisynaptic) and the degree of convergence of different inputs.

Along all three pathways, one cell type is contacted twice: lamina III pyramidal cells along the first pathway, lamina VI pyramidal cells along the second pathway, and lamina IV cells along the third pathway (see Fig. 3*C*). These recurrent excitatory connections can be seen as positive-feedback loops. Like the thalamocortical feedback loops, they could be potential causes of rhythmic, reverberating activity.

Long-distance connections (*dashed lines* in Fig. 3*C*) are involved in the activation within lamina II (sink c) and in the activation within lamina V (sink f) (see above). They are definite demonstrations that the retinotopic organization of the afferent activity is overcome even within the primary visual areas. These lateral dissipations and the concomitant high convergences of afferent activity from near and distant regions indicate that higher-order processing occurs even within primary areas 17 and 18 (see also sect. III*B*). Anatomical demonstrations of intra-areal tangential long-distance connections are in accordance with these findings (59, 88, 89, 179, 259, 298).

Three different classes of Y-type afferents are postulated according to the CSD results. One class of fast-conducting afferents activates area 18. This activity is barely affected at the thalamic relay station (see III*A2*). The second and independent class of slower-conducting Y-type afferents leads to the activation of lamina IVa and the supragranular layers of area 17. This afferent activity is strongly affected by the thalamic relay. A third class of very fast conducting Y-type afferents causes the intracortical evoked inhibition by activating inhibitory interneurons (279, 307, 308). These latter afferents may be identical for both areas. They are probably the Y-type afferents that were found in anatomical studies to bifurcate and send collaterals to areas 17 and 18 (83, 85). The above conclusion that most Y-type afferents to area 17 and area 18 belong to different classes disagrees with several single-unit studies (113, 279, 294), but agrees well with recent anatomical studies (85, 114, 162).

A quantitative comparison of the CSDs from the two primary visual areas reveals that the supragranular activity dominates in area 18, but the infragranular activity dominates in area 17. Anatomically the supragranular layers are also thicker in area 18, whereas the infragranular layers are thicker in area 17 (227). Because the supragranular pyramidal cells project to other cortical areas (87), these quantitative differences suggest that area 18 is more engaged in the relaying of visual information onto secondary, further abstracting areas. In area 17, on the other hand, the dominant concern may be the processing of X-type afferent activity within the infragranular

layers. The efferents of the lamina VI pyramidal cells project back to the LGN (87) and thereby regulate this afferent input (e.g., ref. 271). Because essentially all the afferent X-type activity is relayed to the infragranular layers of area 17, and because these layers do not project to higher cortical areas, it seems that all the X-type visual information is processed extensively within area 17. This isolated processing of the X-type information may be related to the supposition that the X system and area 17 are phylogenetically younger than the Y and W systems and area 18 (266, 282). [Model considerations about perception of forms by humans (90) are well in line with the above conclusion that the low-resolution Y-type visual information is processed also in secondary, further abstracting cortical areas; the high-resolution X-type information, on the other hand, is not necessary to explain higher visual brain functions.]

In summary, the CSD analysis of electrically evoked field potentials in the cat visual areas 17 and 18 has revealed several new facts about the intracortical processing of primary afferent information. It has revealed the laminar segregation of the X- and Y-type afferent inputs, and the lamina-specific intracortical transmission of excitatory activity along distinct pathways. It has demonstrated physiologically that the retinotopic organization is overcome already within the primary areas. The independence of the Y-type afferents to areas 17 and 18 has been revealed. The effects of inhibition on the relays of excitatory activity in the thalamus and in cortex have been assessed quantitatively.

B. Visually Evoked CSDs

Most visually evoked field-potential profiles were recorded simultaneously in all cortical depths with a multiple electrode. These electrode arrays consisted of individual micropipettes, glued together so their tips were aligned and equidistant at 150 or 200 μm, respectively (error $\pm$ 10%). The applied visual stimuli were strobe flashes, Ganzfeld changes of luminance, appearance and disappearance or reversal of a grating (variable spatial frequencies and orientations), moving gratings, and moving bars. The luminance range of the Ganzfeld and the gratings was 3–8 cd/m^2. Several examples of visually evoked CSDs are shown in Figures 4 and 5.

1. Comparison of electrically and visually evoked CSDs

Qualitatively the CSDs evoked by the various types of visual stimuli are very similar to the CSDs evoked by electrical stimulation of the primary afferents. The series of CSDs shown in Figure 4 demonstrates this finding; as described above (see sect. III*A* and Fig. 3*B*), early sinks are apparent in input layers IV and VI (sinks a, d, and e) in all CSDs. A sink in layer III (b) follows, slightly delayed, and then two more dissipated sinks in layers

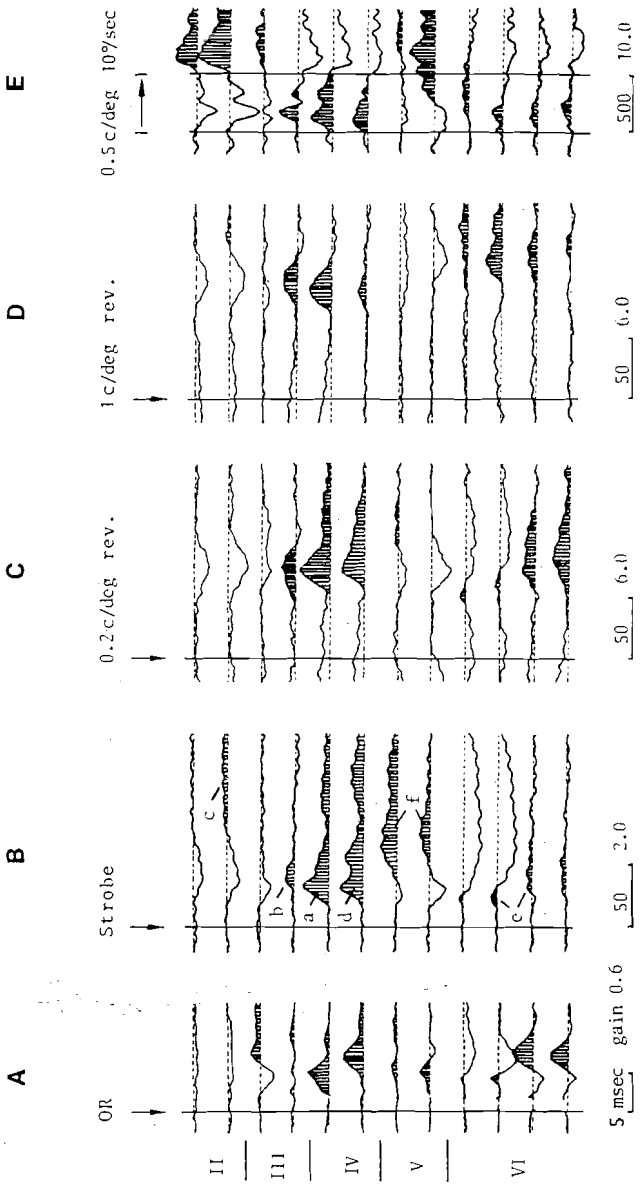

II and V (c and f) follow, with considerable delays. The depth regions of the corresponding sources are also identical in all these CSDs. Quantitatively these CSDs differ in latencies, durations, and amplitudes by factors of 10–100 (note the different time scales and gains shown below the CSDs in Fig. 4).

The qualitative similarities of the sink and source distributions strongly suggest that the visually evoked CSDs reflect the same types of excitatory synaptic ensemble activities along the same intracortical pathways as the electrically evoked CSDs (sect. III*A3*; Fig. 3*C*). This analogy is plausible, because the cortical interconnectivities for the processing of afferent excitatory activity are the same, whether the activation is elicited by electrical or by photic stimulation. Aside from the similarity of the CSDs, several further arguments corroborate the suggestion that the naturally evoked CSDs are also caused by excitatory synaptic activity; contributions from APs are even less likely for these CSDs, because the visual activation is less coherent (see Table 1). Significant contributions from inhibitory synaptic activity could be ruled out, because the visually evoked CSDs, like the electrically evoked CSDs, were consistently enlarged after application of picrotoxin and were consistently diminished after an additional injection of pentobarbital. Contributions from glial cells become more likely the slower the time courses of the events are (sect. II*C1*). Because glial cells redistribute K^+, they should turn sink/source dipoles into more symmetric source/sink/source distributions. No such alterations were observed, however, even in the slowest CSDs (e.g., the dipoles that extend over layers II–IV; Fig. 4*E*).

Because the temporal dissipation of CSDs due to synaptic activation does not cause any cancelling of membrane currents (see sect. II*C2*), the effectiveness of the various stimuli in activating cortex can be assessed by comparing the areas (i.e., the integrals) of corresponding sink peaks. For the monosynaptic sinks in layer IV of area 17, such a comparison reveals that electrical stimulation and all the abrupt visual stimuli (strobe flash, Ganzfeld luminance change, grating on or off, and reversal) are about equally effective; but moving gratings are five times more effective in activating area 17. With respect to area 18, electrical stimulation is two to three times more effective than the applied natural stimuli.

FIG. 4. Electrically and visually evoked current source-density (CSD) distributions in area 17, recorded with a 16-fold multielectrode (intertip spacings Δz = 150 μm; differentiation grid $n \cdot \Delta z$ = 300 μm). Recording region corresponded retinotopically to area centralis. Stimuli and number of responses averaged were: *A*, electrical stimulation of optic radiation, 20 sweeps; *B*, strobe flash, 200 sweeps; *C*, reversal of 0.2 cycle/deg grating (square wave, 40% contrast), 150 sweeps; *D*, reversal of 1 c/deg grating (square wave, 40% contrast), 200 sweeps; *E*, movement of grating (0.5 c/deg, square wave, 40% contrast, velocity 10°/s), 200 sweeps. Time of abrupt stimuli and movement onset and offset are indicated by *vertical bars*. Sinks corresponding to excitatory synaptic relays are *shaded*. Time scales (in ms) and gain (relative units) are given below CSDs. Borders of cortical laminae are indicated at *left*. All CSDs are qualitatively similar (monosynaptic components a, d, and e; polysynaptic components b, c, and f), although their time courses and amplitudes differ by 1 or 2 orders of magnitude.

Analogous to the quantitative differences in the monosynaptic activities are the relative sizes of the late polysynaptic sinks in layer II (e.g., Fig. 4*E* compared with Fig. 4*A-D*). This means that the Y-type afferent input is processed farther along the first pathway to the supragranular layers the larger it is in toto, no matter whether it arrives in cortex within 2 or 100 ms. This implies considerable latitude for temporal summation of inputs at the first two intracortical relay stations along this pathway.

Although all of the visual stimuli were "nonadequate" stimuli (i.e., nonoptimal with respect to the receptive fields of most or all of the neurons in visual cortex), their potency of activation agrees well with single-unit results. Whereas adequate stimuli cause rigorous responses in the few cells with corresponding receptive fields (~2% of the cells, on the average), the electrical and the nonadequate visual stimuli evoke few spikes in most of the cells.

2. Stimulus-specific properties of visually evoked CSDs

In many recent studies, several laminar specificities were revealed for the receptive fields of single units (e.g., refs. 16, 80, 86, 105, 149, 165, 207, 209). Therefore, quite large lamina-specific differences evoked by different types of stimuli were also expected in CSDs. The comparison of many homologous series of visually evoked CSDs (3,000 averaged profiles were recorded) revealed, however, that the specific properties of the stimuli are reflected only in minor modulations of the basic processing pattern (described above and in sect. III*A3*). These modulations are briefly outlined here. The main conclusions are summarized in Figure 6.

a) Abrupt stimuli. An increase of the luminance step of an abrupt stimulus leads to a CSD that has a shorter latency, is compressed in time, and has higher amplitudes (Fig. 4*B* and *C* may be taken as examples). All these effects may be attributed to the shorter latency and the higher coherence of the afferent input (e.g., ref. 29).

Increasing the contours of an abrupt stimulus (compare Fig. 4*C* and *D*) leads to a differential increase in the onset latencies of the sinks in layers IV and VI. Compared with the sink in layer IV, the sink in layer VI has a longer latency (Fig. 4*D*), whereas it has a shorter latency when the stimulus contains few or no contours (Fig. 4*B* and *C*). Usually both these sinks initially draw current mainly from above, and later they draw current from above and from below. For both sinks, the initial phase is more pronounced with less contours, the later phase is more pronounced with contour-rich stimuli. Furthermore, the sinks in the supragranular layers are slightly smaller in amplitude with contour-rich stimuli. All these contour-dependent modulations were equally apparent in areas 17 and 18.

Because the afferents from the A laminae of the LGN contact laminae IV and VI via collaterals (57, 88, 163, 164), the differences in onset latencies

of the sinks in laminae IV and VI must be caused by activations from other types of afferents. Y-type afferents from the C laminae of the LGN and from the medial interlaminar nucleus (MIN) may account for the earlier onset of the sink in lamina IV; these fibers are fast conducting and terminate exclusively in upper layer IV (see Fig. 6: g in area 17 and a in area 18; 163, 164). The earlier onset of the sink in lamina VI (if the stimulus contains only few contours) is not attributable to primary afferents, because none of them terminate exclusively in layer VI. Arguments given below (sect. III*B2d*) suggest that fast-conducting afferents from area 18 could be the causes of these early sinks (see Fig. 6: h in area 17 and e1 in area 18).

With the exception of this yet unidentified input, the modulations in area 17 may be attributed to differences in the proportions of afferent Y- and X-type inputs: contour-rich stimuli activate relatively more X-type afferents; correspondingly the activity along the second pathway (d, e2, and f in Fig. 6) is pronounced, whereas the one along the first pathway (a–c in Fig. 6) is attenuated. Because the modulations caused by increasing contours are identical in area 18, a subdivision of the Y-type afferents to area 18 into contrast-specific and contour-specific subgroups, analogous to the Y-type and X-type afferents to area 17, is highly likely. In Figure 6 this subdivision of the Y-type afferents to area 18 has tentatively been assumed to correlate with different origins of the fibers, LGN A laminae versus LGN C laminae and MIN. The focused termination of the Y-type afferents from the LGN A laminae in area 18, as suggested by a degeneration study (263), is indeed a characteristic feature of X-type afferent terminals in area 17 (57). A mediation of the contour-specific activity in area 18 via area 17 can be ruled out, because it occurs slightly earlier in area 18.

b) Moving gratings. Examples of responses to moving gratings are shown in Figures 4*E* and 5*B*. The most prominent feature of this type of stimulus is the onset of movement. With increasing velocity (and to some extent also with decreasing spatial frequency of the grating), the latency to onset of the early sinks in the input layers is reduced, and the successive intracortical events follow more closely. In area 17 the sinks in layer IV (a and d in Fig. 5*B*) become smaller; but an early sink at the border of laminae III and IV, with a corresponding source in layer II, becomes apparent at higher velocities (g in Fig. 5*B*). The early component of the sink in layer VI, which draws its current exclusively from above (h in Fig. 5*B*), becomes much larger, whereas the later part of this sink (e in Fig. 5*B*) becomes smaller. At velocities >50°/s, only the large component h and the smaller component g are evoked. In area 18, in contrast to area 17, the phasic sink in layer IV (component a) becomes larger in amplitude, the tonic component (d) becomes smaller. The sink in layer VI (component e) is not increased at higher velocities, but like component a, becomes more transient. [The dipolar CSD component a in area 18 is the main cause of the well-known lambda wave at the cortical surface (151).]

During the movement of the grating, the sinks in the input layers are modulated differentially in the two areas. In central area 17 the sustained components d and e are modulated by the individual bars of the grating, in the velocity range of ~5-20°/s. In area 18 the sinks in the input layers become more phasic with increasing velocity; a rhythmic modulation at ~10 Hz steadily increases in the velocity range of ~5-20°/s. This steady increase in modulation apparently corresponds to a decrease of the tonic components d and e and an increase and recurrence of component a; the phasic part of component e recurs like component a, but does not increase in amplitude. At velocities of 20-60°/s, phasic sinks with similar amplitudes occur repetitively at a frequency of 10 Hz until movement stops. At still higher velocities (investigated up to 300°/s), these sinks become even more phasic; concomitantly the first sink in lamina IV (due to the onset of movement; see above) increases in amplitude, whereas the succeeding sinks decrease in amplitude.

The cessation of movements at low and intermediate velocities causes the activation of components c and f in area 17; these components are evoked, regardless of whether they were already activated by the movement onset (see Fig. 4*E*). If the grating was moved at higher velocities, however, the movement stop evoked sinks in the input layers. The transition between these two types of responses to movement stop depends on the velocity as well as the spatial frequency of the grating (4°/s for 1 cycle/deg gratings, 20°/s for 0.5 c/deg gratings, 30-100°/s for 0.2 c/deg gratings). In area 18 the cessation of a movement at low or intermediate velocities does not evoke any response. But if a grating moves at very high velocities for at least 200 ms, the movement stop causes a response. This response is identical to the corresponding response to movement onset. [These findings agree well with the properties of lambda components (151).]

The specific response to stop of slow movements in area 17 was the only response to natural stimuli that did not start with sinks in the input layers. Therefore it cannot be attributed to specific afferent activation. A likely explanation for the generation of these activity components of types c and f may be a release of the preceding relay stations (b and d and/or e2 in Fig. 6) from inhibition. The corresponding tonic inhibition during the preceding movements is probably caused by type X afferents, because this effect occurred only in area 17, was more pronounced in the central regions, and was only related to gratings with high spatial frequencies (Fig. 6, *dotted connections at left*). The range of parameters at which this type of movement-stop response occurs corresponds well with the optimal parameters for the occurrence of a psychophysical phenomenon, the waterfall or motion aftereffect (229). Therefore a correlation between these two phenomena is strongly suggested.

c) Moving bars. Because the one-dimensional CSD method was applied, sinks and sources, which are localized with respect to the horizontal direction, are not adequately focused by this analysis. Horizontally the sinks and sources are not resolved according to their locations, but only according to the lateral decay of the corresponding locally evoked potential fields. When the response to a moving bar is recorded at a certain cortical site, this "delocalization" is equivalent to temporal dissipation of the sinks and sources. Figure 5*A* shows such a response.

When a bar moves over the receptive field of the cortical recording area (Fig. 5*A*, *vertical arrow*), sinks appear in the input layers and in layer III. Usually the onset of the sink in layer VI precedes the onset of the one in layer IV. These components are followed by sinks in layers II and V. Sinks of smaller amplitude in these same layers usually also precede the local activations. Furthermore, if the location of the receptive field is far from the bar at movement onset, a small response to this onset is also recognizable (see Fig. 5*A*).

Assuming, according to single-unit studies, that the sink in layer IV is essentially caused by local retinotopic activation, the delocalization of the CSDs due to the inadequacy of the method can be roughly estimated. The temporal extents of the sinks in layer IV (according to the velocities of the moving bars) correspond to angular extents of 1-5°. This range corresponds to ~5 mm in cortex (310, 311).

The cortical responses to moving bars can largely be interpreted on the basis of the general pattern of activation described in the preceding sections: local afferent activations in the input layers, and then in layer III, are succeeded by activations in layers II and V. The fact that sinks in layers II and V also precede the local activations agrees well with the finding that long-distance connections contribute to these sinks (see sect. III*A3*). The retinotopically noncorresponding activation of the input layers at the movement onset of a bar, however, is a finding that could not be disclosed by the types of visual stimulation described above.

d) Retinotopically noncorresponding activations. The retinotopic correspondence or noncorrespondence of the various CSD components was assessed

FIG. 5 (see following pages). *A*: CSDs in area 17, recorded with 16-channel multielectrode [Δz = 150 μm; $n \cdot \Delta z$ = 300 μm; 200 sweeps averaged; sinks are *shaded;* laminar borders indicated at *left;* time scale (in ms) and gain (in relative units) indicated below]. Stimulus was a moving bar (velocity 20°/s). When bar moved over receptive field (*vertical arrow; cross* in the *inset*), sinks were evoked in input layers and in layer III. They were preceded and followed by sinks in layers II and V. Movement onset also evoked response. *B-D*: CSDs in area 17, evoked by movement of grating (0.2 c/deg, square wave, 40% contrast), subtending 40 × 50° of visual field (*B*), subtending central 12° (*C*), sparing central 24° (*D*), as indicated in *insets*. Respectively, 200, 500, and 400 sweeps were averaged; otherwise, parameters and conventions as in *A*. Various components of CSD in *B* can be attributed to retinotopic versus nonretinotopic activations according to presence or absence in CSDs in *C* and *D*. *E-I*: CSDs in area 18, recorded with 12-fold multielectrode (Δz = 200 μm; $n \cdot \Delta z$ = 200 μm; 200 sweeps averaged). Stimulus was abrupt Ganzfeld increase of luminance (3-8 cd/m^2), in 40 × 50° of visual field (*E*), in the central 24° (*F*), in central 12° (*G*), in 40 × 50° of visual field except for central 12° (*H*) and central 24° (*I*), as indicated in *insets*. Receptive field was 7° lateral and 7° below area centralis (*cross* in *insets*). Conventions as in *A-D*. For comparison, peak latencies of retinotopically evoked components a, b, and e (CSD in *G*) are indicated by *vertical bars* in all CSDs in *E-I*. Retinotopically evoked components a and b (CSD in *G*) are not evoked by peripheral stimulation (CSDs in *H* and *I*). Longer-latency components evoked in these layers by retinotopically noncorresponding stimulation (CSDs in *H* and *I*) are not present (or much smaller) in CSDs evoked by central or whole-field stimulation (CSDs in *E-G*).

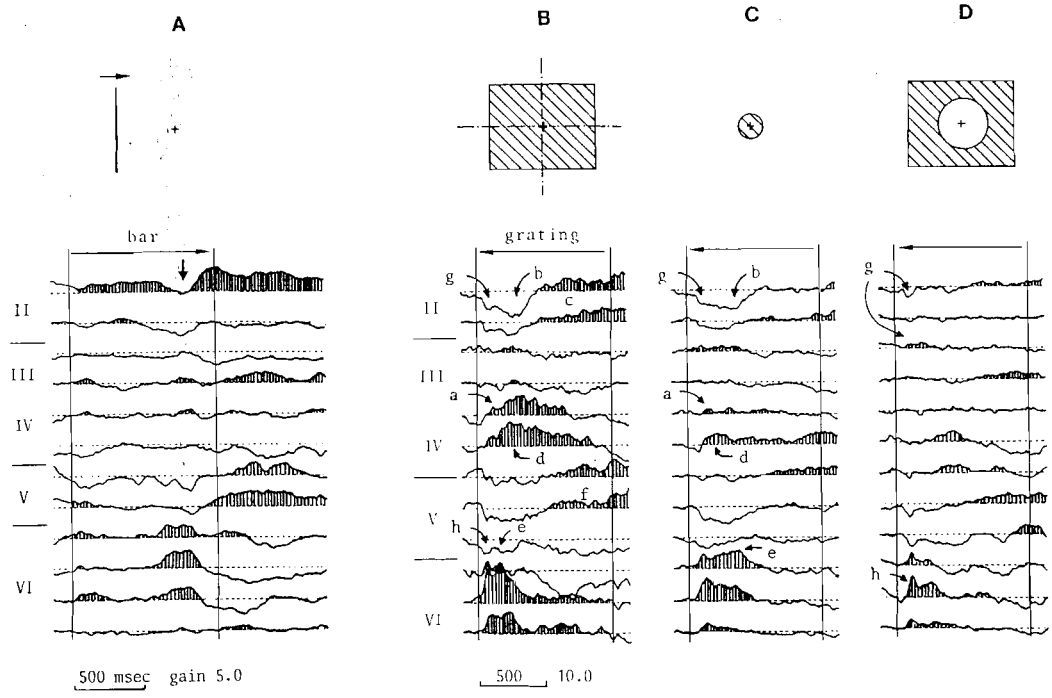
A
B
C
D
bar
grating
II
III
IV
V
VI
a
b
c
d
e
f
g
h
500 msec gain 5.0
500 10.0

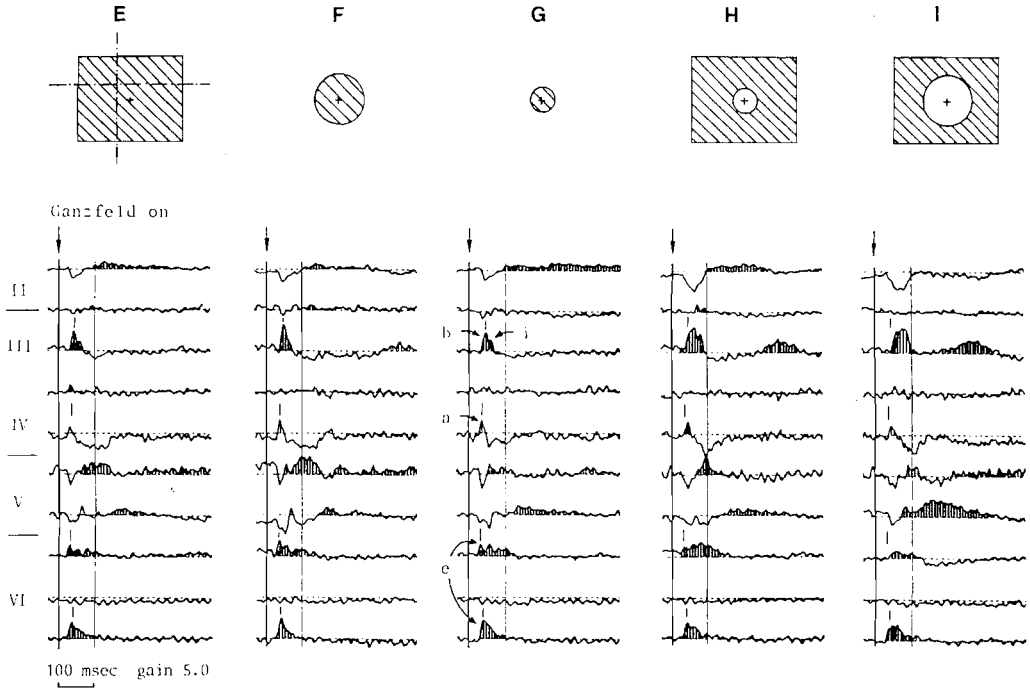
E
F
G
H
I
Ganzfeld on
II
III
IV
V
VI
a
b
e
i
100 msec gain 5.0

by restricting the visual stimuli either to a region 12 or 24° in diameter, centered on the receptive field of the cortical recording region, or to the periphery, sparing the central 12 or 24° (see insets in Fig. 5). The differences in visual-field angles of these restricted stimuli are much larger than the resolution of the one-dimensional CSD method (~5° of visual angle). Examples of responses to these restricted stimuli are shown in Figure 5*B–D* for a moving grating and in Figure 5*E–I* for an abrupt luminance increase.

Retinotopic correspondence was fairly well attributable to the relay components a, b, and d in both areas 17 and 18 (see Fig. 5*C, D, F–I*). The components g, h, and e, evoked in area 17 by the onset of movements, however, are nonretinotopic activations: component g is evoked about equally well by movements in the receptive field and in the far periphery; component h is more pronounced if the periphery is stimulated; component e is more pronounced if the receptive field is stimulated (see Fig. 5*C, D*). The responses to abrupt stimuli indicate that the contour-related and the luminance-related parts of component e differ slightly: component e2 is more directly related to retinotopy than component e1.

These results agree well with the previously mentioned correlations of the various components with monosynaptic activations by different types of primary afferents and with intracortical connections (see Fig. 6), if high retinotopic order is assumed for the afferents from the A laminae of the LGN and low retinotopic order is assumed for the afferents from the C laminae and the MIN (in accord with single-unit data; 159). Only the attribution of component a in area 18 does not fit into this concept, since it was found to be retinotopically evoked. (A further differentiation of the afferents to area 18 may solve this discrepancy; see ref. 190.) The intracortical connections that generate sink h, must come predominantly from a cortical region that represents the peripheral visual field. The border region of area 18 is a likely candidate, because this region projects to area 17 (138, 322) and because the cells in this region respond best to very high velocity movements (257). The primary afferents activating this cortical region come predominantly from the MIN (83, 114, 223, 262).

Although the components a, b, d, and e2 could be attributed to retinotopic activity, large-amplitude sinks are evoked in the same layers also by retinotopically noncorresponding stimuli. The interrelations between these sinks are very similar to the CSDs evoked by retinotopic activation, only the onset latencies are longer. The delays are in the range of ~10–40 ms for responses to abrupt stimuli and up to several hundred milliseconds for moving gratings (compare Fig. 5*C, D,* and *F–I*). The delayed components are not activated equally well by whole-field stimulation (compare Fig. 5*E* and *I*). These observations strongly suggest that intracortical long-distance connections cause these activations and that they are inhibited, if the stimulus extends over the whole visual field.

Intracortical electrical stimulation has already revealed long-distance connections (see sect. IIIA). These stimulations within the supra- or the infragranular layers predominantly evoked components c and f, but small

preceding sinks in the input layers were also evoked (197). With natural stimuli, applied in retinotopically noncorresponding regions of the visual field, the delayed intracortically mediated CSDs are more like the whole-field responses (with the final relay stations being less predominant). This agrees well with the anatomical findings about intra-areal tangential long-distance connections, which run predominantly in the two bands of Baillarger and terminate predominantly within the input layers or at their borders (59, 82, 138, 259). [Only 5–30% of the terminals in the input layers belong to primary afferents (32, 84, 163, 284).] Apparently the activity that is spread out in the cortex along these tangential fibers is processed at the terminal sites along the same main interlaminar pathways as the retinotopically evoked primary afferent activity.

The mutual lateral inhibition preventing the lateral spread of retinotopic activation, if the whole visual field is stimulated, must be fast, because the delay of activation from distant cortical sites may be as small as 10 ms (including the conduction time). Therefore the strong short-latency inhibition mediated by the fastest conducting Y-type afferents (279, 307, 308) is the most likely type of inhibition responsible for this retinotopic focusing of cortical activation. The focusing effect of inhibition has been demonstrated in single-unit receptive-field studies (44, 260, 275, 309). It has been concluded from anatomical studies that lateral inhibition is the predominant type of inhibition in the cortex (e.g., refs. 50, 299). Finally, intracortical long-range mutual inhibition was also suggested by the results of a psychophysical study (321). Mutual lateral inhibition is indicated in the center of Figure 6.

3. Summary of information gained from CSD analyses

Figure 6 summarizes the information gained about the intracortical processing of visually evoked afferent activity. It is composed according to the arguments mentioned above from visually evoked CSDs and by correlation with related anatomical and single-unit data.

The basic intracortical pattern of activation revealed by electrically evoked CSDs (see sect. IIIA*3* and Fig. 3*C*) could be further differentiated. In both areas, three different types of afferents and intracortical processing circuits could be distinguished according to their activation by specific features of the visual stimuli. Although every type of visual stimulus activates all three of these processes, the differential strengths as well as the speed of each process depend on the specific features of the stimulus. As with electrical stimulation, a close similarity between area 17 and area 18 with respect to the intracortical processing of afferent information was apparent with the visual stimuli.

Contour-specific information and slow movements are processed predominantly within lower layer IV and the infragranular layers. These layers are thicker in area 17 than in area 18, and the corresponding afferents to area 17 are numerous (all of the X-type afferents), whereas the corresponding

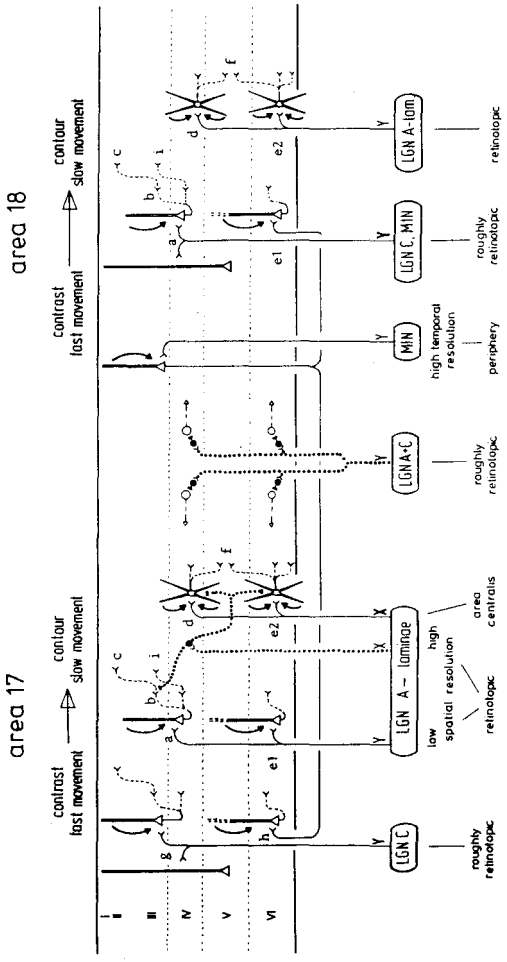

FIG. 6. Summary diagram of different types of intracortical circuits and different types of primary afferents in area 17 and 18, as suggested by visually evoked CSDs (see sect. III*B*). Characteristic features of stimuli that dominate activation of circuits are indicated *above*; retinotopic correspondence of activity is indicated *below*. Afferents causing intracortical inhibition are *dotted*. Three circuits from *left to right*, in each area, process afferent information with progressively higher spatial resolution and progressively lower temporal resolution (progressively slower processing). Phylogenetic age of these circuits in either area probably progressively decreases from *left to right* (see sect. III*A3*).

Y-type afferents (from the A laminae) to area 18 are few (85, 114). Therefore area 17 predominates in the processing of this type of information. The processing of high-acuity information is even totally confined to the infragranular circuitry of area 17 (e.g., ref. 15). Also, the signaling of the cessation of slow movements is confined to area 17 (presumably caused by the release from X-type inhibition).

Contrast-specific information and intermediate velocities are processed predominantly within upper layer IV and the supragranular layers in both areas. The lamina V pyramidal cells are incorporated in this circuitry. In accord with a general topographic rule, these cells have their somata in an infragranular layer, because they project this afferent and processed information out of cortex (e.g., to the superior colliculus; 87). According to the laminar extents and the numbers of corresponding primary afferents, area 18 predominates in the processing of this type of information. Afferent information about very high velocities, and partly also about abrupt, large luminance changes, activates cells at the border of laminae IV and III (possibly totally within lamina III). This information is processed within the supragranular layers, but it is also relayed down to layer V.

The contour-specific processes are activated in a well-localized manner at the retinotopically corresponding sites (components d and e2). The activated contrast-specific processes are slightly less localized (components a and e1 in area 17). The fast-movement components are activated in a rather delocalized manner even at the monosynaptic level (components g and h in area 17 and a fraction of the components a and e1 in area 18). The localized afferent contour- and contrast-specific information becomes delocalized at relays c and f, respectively. If the strong mutual lateral inhibition (mediated by fast Y-type afferents from the LGN) is prevented by restricting the visual stimuli, the local afferent information is spread tangentially within the input layers, thus activating the corresponding circuits all over the area.

In contrast to CSD studies (and studies of evoked potentials; see refs. 45, 47b, 129, 315), extracellular single-unit investigations apparently do not assess the polysynaptic delocalized states of intracortical processing (e.g., refs. 119, 120, 258). Recent studies suggest that they capture only monosynaptically evoked APs generated by components a, d, e, and g (185, 302). These monosynaptic activations, together with the concomitant lateral inhibition, apparently determine the receptive-field properties of the individual neurons (185).

IV. CURRENT SOURCE-DENSITY ANALYSIS OF PRIMARY EVOKED POTENTIALS IN CAT PERICRUCIATE CORTEX AND GENERALIZATION TO OTHER CORTICAL AREAS AND SPECIES

The CSD studies outlined in the preceding section revealed gross similarities as well as subtle differences in two closely related sensory cortical areas. In this section, several CSD and related studies from other cortical

areas are reviewed, and the similarity of the primary activations in different neocortical areas, as revealed by field-potential studies, are demonstrated.

A. CSDs in Cat Pericruciate Cortex

Towe et al. (306) analyzed potentials evoked by electrical stimulation of the contralateral forepaw in area 4γ of the cat before and after topical application of strychnine. Hoeltzell and Dykes (112) made three-dimensional CSD analyses of field potentials in the cat somatosensory cortex. They used abrupt mechanical stimuli delivered to the forearm. An early detailed study of electrically evoked primary potentials by Amassian et al. (5) is closely related to these CSD studies. These authors recorded the depth profiles of the primary somatosensory evoked potentials and interpreted them according to the basic ideas of the CSD method.

The CSDs of pericruciate cortex (see Figs. 6A2 and 7A of ref. 306) as well as the proposed corresponding circuits (see Fig. 4B1 of ref. 306 and Fig. 18 of ref. 5) are very similar to the results obtained from visual cortex (see Fig. 3*B, C*). Fast-conducting afferents terminate at a middle depth of the cortex (predominantly in layer III in precentral cortex; 296). Slower-conducting afferents terminate slightly deeper. The fast afferent activation (evoked by "on-focus" stimulation of the topographically related cutaneous site; 306) induces a source/sink dipole within layers II and III. This dipole moves gradually upward during the 5–10 ms of its duration. Towe et al. (306) and Amassian et al. (5) attribute this upward movement to upward spread of activity from cell to cell. Therefore this dipolar component appears to correspond exactly to the dipoles marked a and b in Fig. 3*B*. [Due to temporal dissipation, these two components merge into one in visually evoked CSDs as well (see sect. III*B*).]

The afferent activation via the slower afferents causes a weak and variable source/sink/source distribution in the middle layers. Polysynaptic activation generates a similar source/sink/source distribution in layer V (306). These two CSD components correspond well with the components d and f of Figure 3*B;* also, the proposed model circuits responsible for these components are identical in both areas (see Fig. 4B of ref. 306 and Fig. 3*C*).

As in visual cortex, the pericruciate cortex supragranular dipole is succeeded by an inverted dipole in the same depth region (component c in Fig. 3*B*). This component has been attributed to recurrent inhibition and/or to delayed K^+ current by Towe et al. (306). The alternative attribution of this dipole to polysynaptic excitatory activation on the apical dendrites within layer II was not considered by the authors. However, the data as well as the large increase of this dipole after strychnine application (306; see also sect. V*C4*) do not contradict the latter explanation. It was used by Amassian et al. (5) and was also strongly suggested in the visual cortex by several independent arguments (see sect. III). The CSD components, described by Hoeltzell and Dykes (112), appear to be identical with the on-focus evoked supragranular dipole and either of the two variable granular or infragranular components.

The field potentials in pericruciate cortex are another demonstration of a closed-field arrangement due to the curvatures of cortex (140). Here, because of the concavity of pericruciate cortex, the cortical surface corresponds to the center of the activated cortical "sphere" and the white matter corresponds to the outer surface of this sphere. This situation is exactly the reverse of the convex sphere of area 17 (see sect. III*A1*). Consequently, while the potentials are large in the deep layers and small on the surface of area 17 (see Fig. 3*A*), they are large in the superficial layers and small in the deep layers in pericruciate cortex (see Fig. 3 of ref. 306).

B. Evoked Potentials and CSDs in Different Neocortical Areas and Species

Landau and Clare (157) made a comparative study of the primary evoked potentials in the somatosensory, the auditory, and the visual cortices of the cat. The potentials were evoked by electrical stimulation of the specific thalamic relay nuclei and were recorded transcortically. The responses in all three sensory areas were found to be similar in shape and time course. They all consisted of three positive peaks followed by one broader negative peak. The differential recovery cycles of the successive peaks and the latency increases on stimulation of the tracts were also found to be identical for all of these evoked potentials. Accordingly the authors concluded that the primary afferents of these areas were similarly fast conducting and that the intracortical activations were similar as well. In a further study, Landau (155) found that purely orthodromic activation of the anterior sigmoid cortex evoked the same potential pattern. By comparison with the intracortical CSDs in area 18, the second and third positive peaks and the negative peak of this characteristic potential could be attributed to granular and supragranular activity, marked a, b, and c in Figure 3*B* (197). The close similarity of the primary evoked responses in the somatosensory and the visual cortex of the cat was confirmed by Morin and Steriade (203), who compared the depth profiles of these electrically evoked potentials in the two areas.

Several CSD studies have been performed in the monkey visual and auditory cortices (143, 183, 198, 208, 211, 314) and in the visual cortex of the rabbit (251). The electrically evoked CSDs in area 18 of the monkey (198) and the electrically and naturally evoked CSDs in the monkey auditory cortex (P. Müller-Preuss and U. Mitzdorf, unpublished observations) were all qualitatively similar to the CSD pattern shown in Figure 3*B*. They consisted of early sinks in the input layers (only in layer IV in area 18; in layers IV and VI in the auditory cortex), followed by sinks in the adjacent layers III and V. In addition a later more-dissipated sink in layer II, corresponding to component c in Figure 3*B*, was apparent in most of these profiles. Only preliminary data are currently available about visually evoked CSDs in area 17 of the monkey (143, 183, 211, 314). Vaughan (314) attributed the earliest

and most prominent sink of the visually evoked CSD to monosynaptic activation in layer IV. Variable results have been published by Rappelsberger et al. (251) about the rabbit visual cortex. The causes for this variability have not yet been clarified. Two of the three displayed visually evoked CSDs do correspond well with the activation pattern found consistently in the cortices of other species (Fig. 5a and c of ref. 251); the primary responses of these two CSDs consist of one dipolar component, located within the granular and supragranular layers. Because the sink of this component moves gradually upward from layer IV to layer III, and because the corresponding source is located above the sink, this primary response seems identical with components a and b of Figure 3*B*.

In summary, although the CSD data about the primary evoked responses in the neocortex of different areas and species are rather scant, they all agree with the CSD and the model circuitry of Figure 3*B*, *C*. In all areas investigated, components a and b appear to be the most prominent and most reliably evoked components. The components c, d, and f are more variable and less reliably evoked. The time course of activation of these successive components, as well as their amplitudes, varies over a wide range. If the primary afferents are stimulated electrically, then the latencies and the peak widths of these components are in the range of a few milliseconds (e.g., refs. 155, 157, 197, 198, 203). These temporal parameters are increased by a factor of 2–10 or more, if natural stimuli are applied (e.g., refs. 194, 211, 251, 314; for a direct comparison of naturally and electrically evoked potentials in somatosensory cortex see ref. 230).

According to anatomical data, the qualitative similarities of primary evoked responses in different neocortical areas and in different species are to be expected: all cortical areas receive fast-conducting specific afferents from specific thalamic nuclei. These afferents terminate predominantly in the middle layers, mainly in layer IV in the koniocortices and mainly in layer III in the other neocortical areas (e.g., refs. 72, 108, 133, 296). In several areas primary afferents also terminate in layer VI. These specific inputs are more prominent in the koniocortices than in the prokoniocortices and are probably all collaterals of afferents to layer IV (57, 108, 164). The basic similarity of the laminar organization and of the lamina-specific cell types have been summarized by Sanides (266). Anatomists have also pointed out that the main intracortical circuitry is identical in different cortical areas as well (e.g., refs. 269, 299). [In several respects the monkey visual cortex fits best into this global scheme of basic interconnections and primary evoked responses, if area 17 is viewed as an intermediate relay (phylogenetically very young) between the thalamic LGN and the secondary cortical visual areas (e.g., refs. 84, 263).]

C. CSDs in Allocortex

Several in vivo and in vitro CSD studies have been performed in the hippocampus (3, 102, 161, 272, 317), whereas only one CSD investigation has been published about the prepyriform cortex (101). In accordance with the large anatomical differences between these two allocortices (266), the CSD results from these two structures differ significantly. In the hippocampus (regardless of which input was stimulated) only monosynaptic activations, probably succeeded by inhibition, were revealed by the analyses of mass action potentials. In this structure, as in the cerebellum, however, significant CSD contributions may arise from coherently evoked antidromic APs. In addition, dendritic APs can also occur (see sect. II*B*, *C*). The CSD study of the prepyriform cortex, on the other hand, revealed mono- as well as polysynaptic excitatory activation components. The model circuitry that resulted from this CSD study and from related single-unit and anatomical data (101) closely resembles the granular-infragranular part of the circuitry of Figure 3*C*, which involves the mono- and polysynaptic activation of layer VI pyramidal cells.

V. RELATION BETWEEN EEG PHENOMENA AND INTRACORTICAL CURRENT SOURCE DENSITIES

The basic circuitry, along which the specific afferent information is processed within the cat visual cortex, could be identified in detail in this well-known cortical structure (see Fig. 3*C* and sect. III). Comparison of corresponding data from other cortical areas strongly suggests that this model of cortical circuitry is equally valid for essentially all neocortical areas (see sect. IV). Furthermore, the same basic circuitry was found to be activated not only by the primary afferents but also via intracortical tangential fibers (see sect. III*B*).

A review of the vast literature about EEG phenomena and their relation to intracortical activity that accumulated primarily in the 1950s and 1960s (see refs. 35, 48, 156, 241, 270) suggests that most of these phenomena are also compatible with activation along this same basic circuitry. From this point of view, various well-known EEG phenomena are reexamined in this section. Most data about EEG-related intracortical activity, however, do not allow as detailed a distinction between the various activation components as the CSD data described in sect. III*A* (see Fig. 3). Therefore the various types of activation are at first grouped in a slightly coarser manner. The nonspecific modulation system is still very poorly understood. Because it is indirectly and/or directly involved in several of the EEG phenomena reexamined in this section, however, it cannot be ignored in this discussion. Its divergent modulating and activating influences on cortex are considered.

A. Components of Cortical Activation and Their Reflection in EEG

If the fine spatial and temporal details of the various neocortical CSD components described in the preceding sections are ignored, they may be grouped into three distinct categories. A fourth category comprises the in-

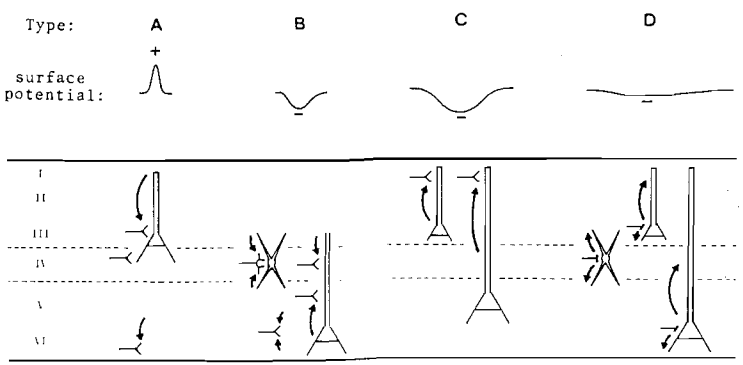

FIG. 7. Schematic diagram of 4 main types of cortical activation and their reflection in surface potential (or EEG). Cell types, synaptic contacts, and currents in extracellular space (*arrows*) are indicated. (For details see sect. VA.)

hibitory activation that does generate field potentials (see sect. II*C3*). Those four types of activation and their reflections in the surface potentials are schematically indicated in Figure 7.

The type A activation causes a dipolar sink/source arrangement, with the sink in the middle depth of the cortex and the source above. This component is essentially due to excitatory synaptic activation of supragranular pyramidal cells at their deeper extremities. The relay stations a, b, g, and i of Figures 3 and 6 are examples of this type of activation. [Only during the fast, coherent electrically evoked activation are the components a and b clearly segregated in time (compare the CSDs of Figs. 3 and 4; see also sect. IV). It is mediated by fast-conducting specific thalamic afferents and/or by intracortical tangential connections (probably the intrinsic fibers of the outer band of Baillarger (59, 84).] The fast coherent activations in layer VI (relay stations e1 and h in Fig. 6) are also considered parts of this type A activation, because they have the same time course and cause dipoles of equal orientation. Type A activation generates a coherent surface-positive potential deflection.

The type B activation causes a sink in the middle depth of the cortex, a low-amplitude source above and a larger-amplitude source below. This component is also caused by excitatory synaptic activation in the middle layers. Compared with the activation of type A, however, relatively more deep pyramidal cells, activated at their apical dendrites in the middle zone, and probably more stellate cells are involved in this type of activation. It is mediated by slower-conducting specific thalamic afferents and/or by intracortical tangential connections (probably predominantly fibers of the inner band of Baillarger; 59). Examples of this type of activation are the relay stations d and f of Figure 3. The slower component of layer VI activation

(e2 in Fig. 6) is considered part of this type B activation, because it has a similar time course and because it also causes a predominantly closed-field component.

Type B activation generates a surface-negative potential deflection that has a slightly slower time course than the type A surface-positive potential. Because of the predominantly closed-field arrangement of the corresponding CSD components, the amplitude of this surface deflection may be rather small, even if the synaptic activation is strong.

The type C activation is identical with the uppermost relay station of Figures 3 and 6. It causes a dipolar sink/source distribution, with the sink in the upper layers of cortex and the source below (in the middle layers). It is due to excitatory synaptic activation of pyramidal cells at the uppermost parts of their apical dendrites. This activation is mediated intracortically (essentially via the type A activation) and involves long-distance connections (probably within layer I; 34, 59). The upwardly directed axon collaterals of the supragranular pyramidal cells are the most likely candidates for the mediation of this type C activation (see, e.g., Fig. 7 of ref. 269; 179). It generates a surface-negative potential of long duration. The strength of this activation and, concomitantly, the amplitude of its surface-negative potential component depend greatly on the general state of excitability of the animal. Accordingly this component is most susceptible to drugs that interfere with the state of excitability (see sect. IIIA*2*; see also, e.g., refs. 43, 186, 306).

A CSD contribution due to inhibitory activity has been identified in a few pathological cases (see sect. II*C3*) and may also arise during slow-wave sleep (e.g., ref. 26). This type D activation generates a slow surface-negative deflection caused by a source in the middle or deep regions and a corresponding sink essentially above. The low amplitudes of the net membrane currents that flow during inhibitory synaptic activity (see sect. II*C3*) and a general lack of lamina specificity of intracortical inhibition (e.g., ref. 279) are supposed to be the main reasons intracortical inhibition does not usually cause significant CSD contributions.

B. Activation Versus Modulation

A dichotomy of the CNS in activating and modulating subsystems has been pointed out by many authors (e.g., refs. 144, 180, 184). The reception and analysis of information from the outside world and the programming of motor patterns are performed by the most recently developed, outermost portion of the CNS, the specific thalamic relay nuclei and neocortex. This type of information processing occurs along rapidly conducting, topographically ordered pathways. Amino acids are the transmitters at the synapses along these pathways. The diffuse network of the central core of the CNS, on the other hand, controls the internal state of the organism. This system is assumed to act very slowly, to use acetylcholine (ACh) and monoamines

as neuromodulators, and to induce gradual changes rather than all-or-nothing effects. Some basic features of this modulatory system have been known for a long time (204), but the underlying physiological mechanisms as well as their anatomical substrates are not yet known; even the most recent reports are very speculative (e.g., refs. 53, 133, 202, 290, 292).

The tonic activity of the ascending reticular arousal system is causally related to consciousness and to the initiation and maintenance of the waking state (135, 180, 204). This tonic activation of the reticular system counteracts the mechanism (or mechanisms) that mediates augmenting, recruiting, and the development of spindles (25, 117, 204, 291, 292). In the cortex the effects of this tonic activation are probably mediated by ACh (53). The background firing of single units in cortex is smoothed during the waking state, and the late phases of evoked responses are enhanced (54, 55, 170). Tonic activation of the mesencephalic reticular formation (MRF) causes hyperpolarization in most cortical cells (139); it does not have any influence on primary evoked responses, but it may reduce a late evoked inhibition (281), and it does suppress afterdischarges (204).

Aside from its tonic action, the brain stem reticular system also appears to be involved in rather phasic phenomena, like the initiation of eye movements (24, 128) and the startling or orienting reflex (e.g., refs. 21, 180). According to single-unit studies, phasic activation of the reticular formation leads to phasic reduction of evoked inhibition in the thalamus, probably preceded by a short increase of inhibition (47, 276). In neocortex, phasic activation of the MRF evokes transient excitation or inhibition in many cells (38, 139, 225, 280, 291). For example, in motor cortex most cells are excited at very short latencies (139); in visual cortex the Y-type cells are more frequently excited, and the X-type cells are more frequently inhibited (136, 225, 280). The response to this phasic activation of the brain stem reticular formation has little effect on the primary responses but enhances secondary responses (76, 204, 273).

It is tempting to speculate that the differential effects of tonic and phasic activation of the brain stem reticular formation are reflections of two qualitatively different functions of this system. The tonic activity may be caused by the nonspecific, tone-regulating system and may act on the specific thalamic and cortical processing systems via neuromodulators. The phasic activities, on the other hand, may be relay components of specific, fast-processing systems. These specific systems are probably involved in the evaluation of the relevance of external stimuli (startle reflex) and in the programming of eye movements.

Also in the thalamus, specific and nonspecific features appear to overlap anatomically to a great extent. Thus the dichotomy between specific and nonspecific thalamic nuclei becomes more and more blurred. Specific thalamocortical afferents, characterized by fast-conducting axons and dense localized terminals in layer IV or III (and VI) of distinct cortical areas, also originate in nonspecific nuclei; thin, nonspecific thalamocortical afferents,

with sparse but widespread terminals in layers other than the specific cortical input layers, also originate in the specific relay nuclei (e.g., refs. 27, 72, 91, 108).

According to their mode of termination in the cortex, the W-type afferents from the LGN belong to the nonspecific type of thalamocortical fibers (57, 164). These afferents make synaptic contacts on spines or dendritic shafts (163). However, no single-unit study could attribute any response property to activation via these afferents, nor was any significant contribution of this W-type activation manifest in electrically evoked CSDs in visual cortex (197). These negative findings may be representative for all the nonspecific thalamocortical afferents, suggesting they all have purely modulatory functions. Consequently all the fast types of cortical activation should be mediated by specific afferents and should therefore start in the specific input layer IV or III (and VI).

C. Natural, Artificially Generated, and Pathological EEG Phenomena

1. Specific and nonspecific primary responses

The activation types A–C of Figure 7, as well as their interconnections (see Fig. 3*C*), have been derived from studies of specific primary evoked CSDs (sects. III and IV). According to the temporal succession of the activation types A, B, and C, the locally generated surface potentials of primary responses consist of a positivity followed by a negativity (e.g., refs. 147, 168, 230). After coherent electrical activation of the primary afferents, the positive component may be resolved into three discrete peaks that reflect the successive events of afferent activation and the monosynaptic and disynaptic activations of type A (e.g., ref. 157).

The type A activation is the most coherent and strategically is optimally evoked at locations close to the soma. The type C activation is least coherent and strategically least effective. Therefore the probability of cell firing is highest during the type A activation, smaller during the type B activation, and very small during the type C activation. Results from several experimental studies that correlated cell responses with the surface evoked potential agree well with this notion (71, 99, 115, 203, 305, 320).

Along with the investigation of visually evoked responses in the cat visual cortex (sect. III*B*), the potential profiles and CSDs of responses to electrical stimulation of the mesencephalic reticular formation and of two thalamic intralaminar regions were also studied. Activation of these sites with stimuli well beyond threshold strength caused rather phasic responses in cortex (see sect. V*B* for corresponding naturally occurring responses). The time courses and amplitudes of these evoked potentials were in the same range as the responses to intermediate or strong visual stimuli. Not only these gross quantitative properties were similar; with respect to spatiotem-

poral details of the CSDs, the specifically evoked and the nonspecifically evoked responses were indistinguishable (U. Mitzdorf, unpublished observations). This close similarity indicates that the same type of intracortical circuitry is activated by the afferent activity from these different regions. Furthermore, from the results of single-unit studies that stimulation of the MRF evokes primary responses in more than 50% of the cells in visual cortex (38, 225, 280), it can be concluded that the activated intracortical mechanisms are not only of the same type but are actually identical.

Direct weak stimulation of the cortical surface evokes a surface-negative field potential (e.g., refs. 1, 48). This response, called direct cortical response (DCR), is apparently identical with the type C activation of Figure 7: it has the same potential and CSD profile as the late component of the primary evoked response (92, 197), and it coincides with excitatory synaptic activation of single cells (40, 167). If the strength of the surface stimulus is increased, or if the stimulus is applied in the middle or deep layers of the cortex, then the surface-negative field potential is preceded (or replaced) by a surface-positive component, the type A activation (40, 92). Yet stronger stimuli evoke a response that looks exactly like the primary response (e.g., ref. 157).

These DCR findings indicate that the model circuitry of Figure 3*C* is of general validity: the relay stations along these circuits are not only the main components for the intracortical processing of specific and nonspecific primary afferent information; the same relay stations are also activated in the same order of succession by totally unspecific, nonselective stimulation of the cortical tissue itself. This identity of the responses evoked by afferents as well as by intracortical stimulation strongly suggests that the pathways along which the specific primary information is processed, involve all the main intracortical excitatory connections and are therefore the main excitatory pathways of cortex in general.

2. *Augmenting and recruiting responses and EEG spindles*

Augmenting responses, recruiting responses, and EEG spindles are closely related rhythmic EEG phenomena (40, 41, 142, 286, 287). They all occur within the same frequency range (5–12 Hz). The trains of events show a characteristic waxing and waning in amplitude. All three phenomena are antagonized by the MRF (117, 290).

Augmenting responses can be evoked by repetitive stimulation of specific thalamic relay nuclei. They develop gradually from primary responses. Compared to the primary responses, the augmenting responses are more dissipated in time, and especially the late component (type C) is more prominent; qualitatively, however, the two responses are very similar (203, 286).

The recruiting response, on the other hand, is commonly viewed as an entirely different phenomenon. In contrast to the augmenting response, the recruiting response lacks the primary surface-positive potential component;

it is assumed to be identical with the type C activation component (61, 91, 142, 286). This response can be evoked by repetitive stimulation of nonspecific thalamic nuclei and is larger in precentral than in postcentral cortex. Projections from the interlaminar nuclei to layer I are assumed to cause the recruiting response (133).

The recruiting response in its pure form, however, seems to occur very rarely or may even be a theoretical extrapolation. The usual type of response to stimulation of nonspecific thalamic nuclei is a mixture of an augmenting and a recruiting component (40, 169, 286); i.e., at least a small activation component of type A or B usually precedes the type C component also in the responses to stimulation of nonspecific thalamic nuclei. Corresponding "specific" thalamocortical afferents from nonspecific thalamic nuclei to the middle layers of precentral cortex have recently been demonstrated (see ref. 91). These facts suggest that the recruiting response may be mediated by the same types of intracortical circuits as the primary or the augmenting responses (see also sect. v*B*). The predominance of the type C activation in the recruiting response may be due to an especially prominent intracortical pathway to layer II of the precentral areas of neocortex. The steady transition of successive spindle events from augmenting-like activations to recruiting-like activations (287) is a further indication that recruiting and augmenting are closely related phenomena that differ only gradually.

The most characteristic feature of recruiting, augmenting, and spontaneous spindles is the steady increase of successive responses or events. This phenomenon is coupled with strong, long-lasting hyperpolarizations (e.g., refs. 117, 290). In thalamic relay cells, these hyperpolarizations are frequently followed by postinhibitory rebound excitations (171). Spontaneous or stimulus-induced synchronizations of such rebound phases in many thalamocortical relay cells are generally assumed to be the main cause of the spindles and the evoked incremental cortical responses (6; for a review of proposed rhythm mechanisms and models see ref. 176).

According to the field potentials, the waxing of successive responses is predominantly due to an increase of the type C component (139, 286, 287). However, if the type C component is mediated intracortically, as suggested above, the postulated thalamic synchronizing mechanisms alone cannot explain the cortical increment phenomenon; instead an additional cortical mechanism must be postulated. The existence of such an independent intracortical mechanism has been demonstrated directly in studies of isolated cortical slabs (e.g., ref. 39) and by studies of cortical responses in animals with thalamic lesions (e.g., ref. 203). Augmenting of properly timed responses was observed in those cortical regions that were disconnected from the thalamus (39, 203). In isolated cortical tissue the postexcitatory inhibition appears to be normal, but postinhibitory rebound activation does not occur, and spontaneous spindling is markedly reduced (39, 73, 145).

These experimental findings and the thalamic synchronizing mechanism may be combined by a rather simple model consideration to explain the

specific increase of the type C component of the cortical response during augmentation: suppression of the reticular activation leads to a reduction of its disinhibitory influence on the thalamus (e.g., ref. 290) and consequently to an increase of amplitude and duration of the intrathalamic inhibition. Due to the corresponding increased average negativity of the membrane potentials, many cells may then switch into an autonomously oscillating state, as recently proposed by Llinás and Jahnsen (171). Because of intrathalamic interactions, many of the otherwise independent oscillators may become synchronized from time to time. However, even if the cells do not reach the autonomously oscillating state, the more effective inhibition (mediated mainly by feedback loops) makes a spontaneous synchronization of the individual cell outputs more likely (176). These thalamic synchronizations cause the spontaneous activity in the thalamocortical afferents to become grouped into coherent volleys, with long phases of extremely low average activity between.

When the first of such a train of afferent volleys reaches the cortex, the excitability states of the individual cortical cells are uncorrelated; therefore the usual primary response and the concomitant inhibition are evoked. The following interburst interval is long enough for the cells to recover fully from the evoked inhibition. When the second burst arrives in the cortex, the states of the cortical target cells are rather synchronized at a low-threshold level. In addition, this synchronization of cortical cell states is augmented by the depression of spontaneous activity in the thalamocortical afferents during the interburst intervals. As mentioned in section III*A2*, the type C activation (which is reflected in the CSD component c) is extremely susceptible to changes in the excitability of cortex. Therefore a synchronization of the cortical cell states will have its largest effect on the type C component. This would explain why the type C component of the cortical response increases most drastically during the waxing phase of the recruiting or augmenting responses and why it increases steadily from the beginning toward the end of a spindle (e.g., refs. 139, 286, 287).

3. Secondary responses and repetitive afterdischarges

Primary cortical responses are usually followed by more waves of activation. Such secondary responses have been described already in the first report about evoked potentials (12). Since then many studies have concentrated on these late evoked responses, and it has become obvious that various types of secondary responses must be distinguished (see, e.g., refs. 76, 304). These distinctions are difficult to assess, however, because the different types of late responses usually occur in admixed form. The clearest subdivision appears to be the segregation of the late responses into the repetitive sensory afterdischarges and the nonreiterative secondary responses (76).

The repetitive sensory afterdischarges are evoked in states with a synchronized EEG and are enhanced by barbiturates (76); they are abolished

during repetitive stimulation of the reticular formation (204). Sensory afterdischarges are closely related to the phenomena of spindling and recruiting (25, 117) or to the alpha rhythm of the EEG (13, 166, 255); but they may also originate in the periphery, e.g., in the retina (316). In a model their appearance could be described by a synchronization of previously uncoupled passive oscillators, because of the primary activation by the stimulus (13).

Such repetitive afterdischarges are apparent in the visually evoked CSDs of the rabbit cortex (251) and have also been recorded during the CSD study of visually evoked responses in the cat cortex (sect. III*B*). They occurred rather consistently when the animal was in a state of deep anesthesia and/or low excitability. The CSDs of the afterdischarges usually show only small sinks in the input layers; i.e., the corresponding activity was type A and B. They usually recurred a few times with successively lower amplitudes and longer intervals (U. Mitzdorf, unpublished observations). These observations agree well with the notion that the repetitive afterdischarges are generated in the thalamus (25, 117) or in the retina (316) and are conducted to the cortex via specific afferents. There this afferent activity is not relayed beyond the first or second steps of activation, because the state of excitability is low.

The nonreiterative secondary responses appear to comprise at least two different phenomena. One type is evoked better if the animal is anesthetized, and this type is enhanced by lesions of the mesencephalon (304). This late cortical activity coincides with late activity in the primary afferents (304). Therefore it is probably caused by the secondary responses of the retinal ganglion cells, which have been described by Grüsser and Rabelo (98). The close similarity between the depth profiles of these secondary responses and the profiles of the preceding primary responses was taken as a further indication that both these cortical activities are of retinal origin (17). Because activation by other afferents and even the nonselective activation by intracortical stimulation cause the same type of response (see sect. V*C1*), this inference need not be stringent. The similarity of the profiles indicates, however, that the primary and these secondary responses involve the same intracortical relay stations.

The alternative type of nonreiterative secondary response is evoked best if the EEG is desynchronized, and it is reduced or abolished by barbiturates (54, 76, 304). It is correlated with activations of the MRF (76, 304), and cholinergic synapses participate in its production (300). The specific thalamus may or may not be involved in this type of activation (76, 304). All the secondary components that have been related to complex brain functions like memory (130) and passive or active conditioning (22, 62, 265) belong to this group. Secondary responses that depend on complex features of the sensory stimulus, like the contour-specific component of visually evoked responses (129, 148), must also be adjoined with this type of secondary response.

No details are known about the intracortical patterns of activation during the secondary responses associated with complex brain functions. However, the spatiotemporal distribution of stimulus-specific secondary responses have

been recorded and identified during the studies of the visually evoked CSDs in the cat visual cortex (U. Mitzdorf, unpublished observations). They too caused the same common type of CSD as the primary responses, with early sinks in the input layers, possibly followed by sinks in the supragranular layers and in layer V.

4. Seizure activity

Seizure activities are pathological phenomena of cell ensembles. They involve spontaneous (or stimulus-induced) phasic activation of many cells and are characterized intracellularly by the paroxysmal depolarization shift (PDS; 188, 189). The neurophysiological mechanism underlying the PDS is still insufficiently known. Present hypotheses relate the PDS with voltage-dependent Ca^{2+} currents and/or with supranormal ("giant") excitatory synaptic activations (e.g., refs. 107, 132, 239).

The hypothesis about the pathological exaggeration of the normally occurring synaptic activation is in good agreement with the results of several recent investigations, in which the depth profiles or the CSDs of interictal and ictal spikes were evaluated. Towe et al. (306) found that the CSDs of electrically evoked strychnine spikes in the cat pericruciate cortex are very similar to the CSDs of the primary evoked responses (see also sect. IV*A*). The sinks and sources of strychnine spikes have larger amplitudes and are prolonged by about a factor of 2. The largest amplitude increase due to the action of strychnine was observed in the supragranular components, i.e., the type A activity and the succeeding type C activity. With high-frequency stimulation (3 Hz) the type C component was found to alternate in amplitude. Since PDSs have also been shown to occur alternatingly in every other response at such high stimulus repetition rates (187), Towe et al. (306) interpreted the large-amplitude version of this type C component as the extracellular reflection of intracellular PDSs.

Kostopoulos et al. (142) compared the intracortical laminar profiles of spindles and spikes of the spike and wave complexes in feline generalized penicillin epilepsy. Because the profiles of both phenomena were very similar, the authors concluded that the penicillin spikes reflected enhanced but basically identical physiological phenomena. These consist of two components—a surface-positive phase followed by a surface-negative phase. These components were interpreted as the reflections of excitatory synaptic activations in the middle layers (i.e., the type A activation of Fig. 7) and in the most superficial region (i.e., the type C activation of Fig. 7).

Surface-positive/negative complexes were also recorded by Jami (127). This type of complex was found to be characteristic of all phases of Metrazol-induced seizures in the cat cortex. Jami correlated single-unit activity with these EEG waves. The average multiunit discharges and the EEG components were found to be interrelated during the interictal periods. The cell discharges increased during the occurrence of the surface-positive component and were slightly decreased during the following surface-negative component. This result agrees well with the notion that the surface-positive component is caused by the excitatory synaptic activation of type A and that the succeeding negative component is due to the excitatory, but rather ineffective, activation of type C. The concomitant reduction of cell firing is probably the result of intracortical inhibition, which is mediated via the type A activation of interneurons and may or may not contribute to the surface-negative deflection. During the tonic stage, the level of unit activity is rather constant and very high. No more correlation with the surface wave is apparent. During this stage, the synaptic relay stations are probably activated in the same manner as during the interictal phase, thereby causing the EEG waves; but now these phasic activations are superimposed on the very high tonic background activity that is autonomically generated in the axons (127). During the clonic stage therefore, the firing rate of the cells is high during the surface-positive component and during the first part of the surface-negative component. This correlation may reflect a slower onset of inhibition or the involvement of more type B activation during this stage, compared with the interictal stage.

In the cat cortex the profiles of seizure spikes are predominantly of the open-field type, caused by dipolar sink/source distributions (142, 306; but see also ref. 100). In the rat (51, 116), rabbit (231, 251), and (at least in certain experimental situations) monkey (289) the spike profiles are predominantly of the closed-field type. Clearly, from analyses of potentials in the rabbit visual cortex, the CSDs of the tonic seizure activities are very similar to the visually evoked primary responses (251). During both events, a sink in layer IV is succeeded by a smaller sink in layer III. Because the sink in layer IV draws more current from below during the seizure activity than during the response to visual stimulation, relatively more of the type B activation appears to be involved in the generation of the seizure spike. According to further analyses (231), the sink in layer IV appears to be the main generator of the large-amplitude potential deflections during all stages of the penicillin-induced seizures in the rabbit visual cortex.

In summary, these few examples of seizure-related depth profiles and/or CSDs from neocortex strongly suggest that phasic seizure activity usually involves the same main pathways of cortex as the primary evoked responses. Aside from reduced inhibition and facilitated synaptic transmission, additional Ca^{2+} currents may cause exaggerations of events. The fact, however, that the CSDs are usually not altered in a qualitative way during seizures suggests that these additional Ca^{2+} currents are triggered by synaptic activations and are restricted to the vicinity of the activated synapses.

Although the usual result of comparisons between paroxysmal and normal cortex activations was a close qualitative similarity, an exception was also apparent: a CSD analysis of potential profiles published by Elger et al. (51) revealed that the first two profiles of their Figure 1 are caused predominantly by a type C component and lack the preceding sink in layer IV. Still, the main input layer IV/III is the most susceptible to penicillin epileptogenesis (47a, 175a).

VI. CONCLUSIONS

A. Complementary Access of CSDs to Brain Function

The CSD method is sensitive to population activities of anatomically ordered ensembles; therefore it is located somewhere between anatomy and physiology. It reveals physiological as well as anatomical aspects of brain function. Although additional anatomical and/or physiological information is necessary to identify the causes of the CSDs (see Fig. 1 and sect. II*C*), CSD results add to the existing body of evidence and reveal independent, complementary information.

The fact that the CSD method is restricted to anatomically ordered ensemble activity to be investigated may be viewed as a limitation. This aspect, however, renders the method optimally suited to reveal the anatomical orders of physiologically distinct processes. Viewed empirically, this is even the main advantage of the method. Because there is evidence that cerebral functions are usually based on spatiotemporal orderliness, there is an abundance of questions waiting to be answered by this method.

The CSD method is especially apt to investigate excitatory synaptic activations, which are the predominant causes of the field potentials (see Table 1). It has advantages over anatomical and histochemical methods because of its assessment of temporal information and information about functional weights of synaptic activations, in addition to the localizations. Its advantage over single-unit recordings is its ability to disclose the sites of synaptic activation; furthermore it bypasses the sampling problem and reveals subthreshold activities. The latter two advantages combined give the CSD method access to activations occurring more than just one relay step beyond the activations that can be seen in single-unit studies (see sect. III*B3*). Finally, field-potential analysis is the only method [besides in vitro applications of the new optical recording method (94)] that gives direct and simultaneous access to spatiotemporal properties of neuronal activities.

B. Information Processing in Neocortex: One Basic Pattern of Activation

One of the conclusions to be drawn from the field-potential data reviewed in sections III, IV, and V is they all agree with the basic circuitry of neocortex shown in Figure 3*C*. Activity in the same circuits can be initiated by natural and artificial stimulation, by specific and nonspecific afferent stimulations, and by intracortical stimulation; it can even be spontaneously evoked during sleep, anesthesia, or epileptic seizures, but also during the performance of complex brain functions. It is the same pattern of activation that causes most of the EEG phenomena.

The sequence of excitation may be followed through completely and repetitively or may be choked at the first or second intracortical relay stations. It may be very short (5 or 10 ms, electrically evoked responses), it may consume 50–300 ms (responses to abrupt visual stimuli, secondary responses, activations from the reticular system, paroxysmal discharges), or it may even take 1 or 2 s (responses to weak natural stimuli, weak secondary responses). The product of amplitude and duration of CSD or potential peaks may be taken as a rough measure of the strength of activation.

The data reviewed in the preceding sections indicate that the strengths of electrically or naturally evoked and spontaneously occurring activities are all of the same order of magnitude. The state of excitability of the CNS is as important a parameter with respect to this measure as the specific type of stimulus. For paroxysmal events, the strength of activation is larger by one order of magnitude.

From single-unit studies of properties other than the specific receptive fields, it is known that a large proportion of the cortical cells are involved in different types of cortical activation. Therefore it is unlikely that different types of information are processed along independent parallel circuits. The different types of activity appear rather to be processed by the same circuitry. This circuitry must involve all the cells and connections of the cerebral region. From this point of view it is not relevant to ask whether a certain cortical cell does or does not participate in a certain type of activation. Each cell, then, is characterized primarily by its position in the circuitry and its safety factors of transmission during the various types of activities. Such safety factors of transmission may be very small in certain cases but may never be zero. This view is incompatible with statements, like the hypothesis put forward by Elul (52), that EEG spindles are generated by synchronization of 10% of the cortical cells. It is in line, however, with an experimental finding by Fox and O'Brian (63) of perfect congruencies between evoked-potential waveforms and firing probabilities.

The specific rigid physical properties of the stimuli from the outside world, as recorded by the receptors, are relayed up to cortex along parallel, rather independent pathways. In the cortex these elementary stimulus features are then blurred beyond recognition after only one synaptic relay (see sect. III*B3*). The code(s) of information processing after this transformation is not yet known, but the field-potential studies have already revealed that this processing is performed in one general routine that involves only three successive synaptic relay steps.

I thank Prof. E. Pöppel, Prof. J. Dudel, Drs. M. Mackeben, K. Nakayama, and Prof. C. Nicholson for valuable discussions of the manuscript, P. Mitterhüsen and R. Beck for typing, and G. Weiler for help with the figures.

This work has been supported by a grant from the Deutsche Forschungsgemeinschaft (Mi 141/4-1).

REFERENCES

1. ADRIAN, E. D. The spread of activity in the cerebral cortex. *J. Physiol. London* 88: 127–161, 1936.
2. ADRIAN, E. D., AND G. MORUZZI. Impulses in the pyramidal tract. *J. Physiol. London* 97: 153–199, 1939.
3. ALVAREZ-LEEFMANS, F. J. Functional synaptic organization of inhibitory pathways in the dentate gyrus of the rabbit. *Exp. Brain Res. Suppl.* 1: 229–234, 1976.
4. ALVAREZ-LEEFMANS, F. J. *A Structural and Electro-*

physiological Study of the Synaptic Mechanisms which Affect the Excitability of the Granule Cells of the Dentate Gyrus in the Rabbit (PhD thesis). London: Univ. of London, 1977.
5. AMASSIAN, V. E., H. J. WALLER, AND J. MACY, JR. Neural mechanism of primary somatosensory evoked potential. *Ann. NY Acad. Sci.* 112: 5–32, 1964.
6. ANDERSEN, P., AND S. A. ANDERSSON. *Physiological Basis of the Alpha-Rhythm.* New York: Appleton-Century-Crofts, 1968.
7. ANDERSEN, P., T. V. P. BLISS, AND K. K. SKREDE. Unit analysis of hippocampal population spikes. *Exp. Brain Res.* 13: 208–221, 1971.
8. ARAKI, T., AND C. A. TERZUOLO. Membrane currents in spinal motoncurons associated with the action potential and synaptic activity. *J. Neurophysiol.* 25: 772–789, 1962.
9. BARRETT, J. N., AND W. E. CRILL. Influence of dendritic location and membrane properties on the effectiveness of synapses on cat motoneurones. *J. Physiol. London* 293: 325–345, 1974.
10. BARTLEY, S. H. Action potentials of the optic cortex under the influence of strychnine. *Am. J. Physiol.* 103: 203–212, 1933.
11. BARTLEY, S. H. Temporal and spatial summation of extrinsic impulses with the intrinsic activity of the cortex. *J. Cell. Comp. Physiol.* 8: 41–62, 1936.
12. BARTLEY, S. H., AND G. H. BISHOP. The cortical response to stimulation of the optic nerve in the rabbit. *Am. J. Physiol.* 103: 159–172, 1933.
13. BAŞAR, E. *EEG-Brain Dynamics. Relation Between EEG and Brain Evoked Potentials.* Amsterdam: Elsevier/North-Holland, 1980.
14. BERGER, H. Über das Elektrenkephalogramm des Menschen. *Arch. Psychiatr. Nervenkr.* 87: 527–570, 1929.
15. BERKLEY, M. A., AND R. BUSH. Intracortical processing of visual contour information in cats. *Exp. Brain Res.* 50: 397–407, 1983.
16. BERMAN, N., B. R. PAYNE, D. R. LABAR, AND E. H. MURPHY. Functional organization of neurons in cat striate cortex: variations in ocular dominance and receptive-field type with cortical laminae and location in visual field. *J. Neurophysiol.* 48: 1362–1377, 1982.
17. BIGNALL, K. E., AND L. T. RUTLEDGE. Origin of a photically evoked afterdischarge in cat visual cortex. *J. Neurophysiol.* 27: 1048–1062, 1964.
18. BISHOP, G. H. Cyclic changes in excitability of the optic pathway of the rabbit. *Am. J. Physiol.* 103: 213–224, 1933.
19. BISHOP, P. O., W. BURKE, AND R. DAVIS. The identification of single units in central visual pathways. *J. Physiol. London* 162: 409–431, 1962.
20. BISTI, S., G. IOSIF, AND P. STRATA. Suppression of inhibition in the cerebellar cortex by picrotoxin and by bicuculline. *Brain Res.* 28: 591–593, 1971.
21. BOWKER, R. M., AND A. R. MORRISON. The startle reflex and PGO spikes. *Brain Res.* 102: 185–190, 1976.
22. BRAZIER, M. A. B., K. F. KILLAM, AND A. J. HANCE. The reactivity of the nervous system in the light of the past history of the organism. In: *Sensory Communication*, edited by W. A. Rosenblith. New York: MIT Press, 1961, p. 699–716.
23. BRECKOW, J., K. KALMRING, AND R. ECKHORN. Multichannel-recordings and real-time current source density (CSD) analysis in the central nervous system of insects. *Biol. Cybern.* 45: 115–121, 1982.
24. BROOKS, D. C., AND M. D. GERSHON. Eye movement potentials in the oculomotor and visual systems of the cat: a comparison of reserpine induced waves with those present during wakefulness and rapid eye movement sleep. *Brain Res.* 27: 223–239, 1971.
25. BUSER, P., AND F. E. HORVATH. Thalamo-caudate-cortical relationships in synchronized activity. II. Further differentiation between spindle systems by cooling and lesions in the mesencephalon. *Brain Res.* 39: 43–60, 1972.
26. CALVET, J., M. C. CALVET, AND J. SCHERRER. Étude stratigraphique corticale de l'activité EEG spontanée. *Electroencephalogr. Clin. Neurophysiol.* 17: 109–125, 1964.
27. CAVINESS, V. S., JR., AND D. O. FROST. Tangential organization of thalamic projections to the neocortex in the mouse. *J. Comp. Neurol.* 134: 335–367, 1980.
28. CHUNG, S. H., T. V. P. BLISS, AND M. J. KEATING. The synaptic organization of optic afferents in the amphibian tectum. *Proc. R. Soc. London Ser. B* 187: 421–447, 1974.
29. CLELAND, B. G., AND C. ENROTH-CUGELL. Quantitative aspects of gain and latency in the cat retina. *J. Physiol. London* 206: 73–91, 1970.
30. COHEN, M. W. Glial potentials and their contribution to extracellular recordings. In: *Handbook of Electroencephalography and Clinical Neurophysiology*, edited by O. Creutzfeldt. Amsterdam: Elsevier, 1974, vol. 2B, p. 43–60.
31. COLONNIER, M. Synaptic patterns of different cell types in the different laminae of the cat visual cortex. An electron microscope study. *Brain Res.* 9: 268–287, 1968.
32. COLONNIER, M., AND S. ROSSIGNOL. Heterogeneity of the cerebral cortex. In: *Basic Mechanisms of Epilepsy*, edited by H. H. Jasper, A. A. Ward, and A. Pope. Boston, MA: Little, Brown, 1969, p. 29–40.
33. COWAN, W. M., AND M. CUENOD (editors). *The Use of Axonal Transport for Studies of Neuronal Connectivity.* New York: Elsevier, 1975.
34. CREUTZFELDT, O. D., L. J. GAREY, R. KURODA, AND J.-R. WOLFF. The distribution of degenerating axons after small lesions in the intact and isolated visual cortex of the cat. *Exp. Brain Res.* 27: 419–440, 1977.
35. CREUTZFELDT, O., AND J. HOUCHIN. Neuronal basis of EEG waves. In: *Handbook of Electroencephalography and Clinical Neurophysiology*, edited by A. Rémond and O. Creutzfeldt. Amsterdam: Elsevier, 1974, vol. 2C, p. 5–55.
36. CREUTZFELDT, O. D., AND U. KUHNT. Electrophysiological and topographical distribution of visual evoked potentials in animals. In: *Handbook of Sensory Physiology. Visual Centers in the Brain*, edited by R. Jung. Berlin: Springer-Verlag, 1973, vol. VII, pt. 3/B, p. 595–646.
37. CREUTZFELDT, O. D., U. KUHNT, AND L. A. BENEVENTO. An intracellular analysis of visual cortical neurones to moving stimuli: responses in a co-operative neuronal network. *Exp. Brain Res.* 21: 251–274, 1974.
38. CREUTZFELDT, O., R. SPEHLMANN, AND D. LEHMANN. Veränderungen der Neuronaktivität des visuellen Cortex durch Reizung der Substantia reticularis mesencephali. In: *Neurophysiologie und Psychophysik des visuellen Systems*, edited by R. Jung and H. Kornhuber. Berlin: Springer-Verlag, 1961, p. 351–363.
39. CREUTZFELDT, O., AND G. STRUCK. Neurophysiologic und Morphologie der chronisch isolierten Cortexinsel der Katze: Hirnpotentiale und Neuronenaktivität einer isolierten Nervenzellpopulation ohne afferente Fasern. *Arch. Psychiatr. Nervenkr.* 203: 708–731, 1962.
40. CREUTZFELDT, O. D., S. WATANABE, AND H. D. LUX. Relations between EEG phenomena and potentials of single cortical cells. I. Evoked responses after thalamic and epicortical stimulation. *Electroencephalogr. Clin. Neurophysiol.* 20: 1–18, 1966.
41. CREUTZFELDT, O. D., S. WATANABE, AND H. D. LUX. Relations between EEG phenomena and potentials of single cortical cells. II. Spontaneous and convulsoid activity. *Electroencephalogr. Clin. Neurophysiol.* 20: 19–37, 1966.

42. CRILL, W. E., AND P. C. SCHWINDT. Active currents in mammalian central neurons. *Trends Neurosci.* 6: 236–240, 1983.
43. CURTIS, H. J. An analysis of cortical potentials mediated by the corpus callosum. *J. Neurophysiol.* 3: 414–422, 1940.
44. DANIELS, J. D., AND J. D. PETTIGREW. A study of inhibitory antagonism in cat visual cortex. *Brain Res.* 93: 41–62, 1975.
45. DOTY, R. W. Potentials evoked in cat cerebral cortex by diffuse and punctiform photic stimuli. *J. Neurophysiol.* 21: 437–464, 1958.
46. DOTY, R. W., D. S. KIMURA, AND G. J. MORGENSON. Photically and electrically elicited responses in the central visual system of the squirrel monkey. *Exp. Neurol.* 10: 19–51, 1964.
47. DOTY, R. W., P. D. WILSON, J. R. BARTLETT, AND J. PECCI-SAAVEDRA. Mesencephalic control of lateral geniculate nucleus in primates. I. Electrophysiology. *Exp. Brain Res.* 18: 189–203, 1973.
47a. EBERSOLE, J. S., AND A. B. CHATT. Laminar interactions during neocortical epileptogenesis. *Brain Res.* 298: 253–271, 1984.
47b. EBERSOLE, J. S., AND B. J. KAPLAN. Intracortical evoked potentials of cats elicited by punctate visual stimuli in receptive field peripheries. *Brain Res.* 224: 160–164, 1981.
48. ECCLES, J. C. Interpretation of action potentials evoked in the cerebral cortex. *Electroencephalogr. Clin. Neurophysiol.* 3: 449–464, 1951.
49. ECCLES, J. C. *The Physiology of Synapses.* Berlin: Springer-Verlag, 1964.
50. ECCLES, J. C. The modular operation of the cerebral neocortex considered as the material basis of mental events. *Neuroscience* 6: 1839–1856, 1981.
51. ELGER, C. E., E.-J. SPECKMANN, O. PROHASKA, AND H. CASPERS. Pattern of intracortical potential distribution during focal interictal epileptiform discharges (FIED) and its relation to spinal field potentials in the rat. *Electroencephalogr. Clin. Neurophysiol.* 51: 393–402, 1981.
52. ELUL, R. The genesis of the EEG. *Int. Rev. Neurobiol.* 15: 227–272, 1972.
53. EMSON, P. C., AND O. LINDVALL. Distribution of putative neurotransmitters in the neocortex. *Neuroscience* 4: 1–30, 1979.
54. EVARTS, E. V. Photically evoked responses in visual cortex units during sleep and waking. *J. Neurophysiol.* 26: 229–248, 1963.
55. EVARTS, E. V. Unit activity in sleep and wakefulness. In: *The Neurosciences*, edited by G. C. Quarton, T. Melnechuck, and F. O. Schmitt. New York: Rockefeller Univ. Press, 1967, p. 545–556.
56. EYSEL, U. T. Quantitative studies of intracellular postsynaptic potentials in the lateral geniculate nucleus of the cat with respect to optic tract stimulus response latencies. *Exp. Brain Res.* 25: 469–486, 1976.
57. FERSTER, D., AND S. LEVAY. The axonal arborizations of lateral geniculate neurons in the striate cortex of the cat. *J. Comp. Neurol.* 182: 923–944, 1978.
58. FESSARD, A. The role of neuronal networks in sensory communications within the brain. In: *Sensory Communication*, edited by W. A. Rosenblith. New York: MIT Press, 1961, p. 585–606.
59. FISKEN, R. A., L. J. GAREY, AND T. P. S. POWELL. The intrinsic, association and commissural connections of area 17 of the visual cortex. *Philos. Trans. R. Soc. London Ser. B* 272: 487–536, 1975.
60. FORBES, A., AND B. R. MORISON. Cortical responses to sensory stimulation under deep barbiturate narcosis. *J. Neurophysiol.* 2: 112–128, 1939.
61. FOSTER, J. A. Intracortical origin of recruiting responses in the cat cortex. *Electroencephalogr. Clin. Neurophysiol.* 48: 639–653, 1980.
62. FOX, S. S. Evoked potential, coding and behavior. In: *The Neurosciences. Second Study Program*, edited by F. O. Schmitt. New York: Rockefeller Univ. Press, 1970, p. 243–259.
63. FOX, S. S., AND J. H. O'BRIAN. Duplication of evoked potential waveform by curve of probability of firing of a single cell. *Science* 147: 888–890, 1965.
64. FREEMAN, B., AND W. SINGER. The direct and indirect visual inputs to the superficial layers of the cat superior colliculus: a current source-density analysis of electrically evoked potentials. *J. Neurophysiol.* 49: 1075–1091, 1983.
65. FREEMAN, J. A. Possible regulatory function of acetylcholine receptor in maintenance of retinotopic synapses. *Nature London* 269: 218–222, 1977.
66. FREEMAN, J. A., AND C. NICHOLSON. Experimental optimization of current source-density technique for anuran cerebellum. *J. Neurophysiol.* 38: 369–382, 1975.
67. FREEMAN, J. A., J. T. SCHMIDT, AND R. E. OSWALD. Effect of α-bungarotoxin on retinotectal synaptic transmission in the goldfish and the toad. *Neuroscience* 5: 929–942, 1980.
68. FREEMAN, J. A., AND J. STONE. A technique for current density analysis of field potentials and its application to the frog cerebellum. In: *Neurobiology of Cerebellar Evolution and Development*, edited by R. Llinás. Chicago, IL: Am. Med. Assoc., 1969, p. 421–430.
69. FREEMAN, W. J. *Mass Action in the Nervous System.* New York: Academic, 1975, p. 175 ff.
70. FREYGANG, W. H., JR., AND W. M. LANDAU. Some relations between resistivity and electrical activity in the cerebral cortex of the cat. *J. Cell. Physiol.* 45, Suppl.: 377–392, 1955.
71. FROMM, G. H., AND H. W. BOND. The relationship between neuron activity and cortical steady potentials. *Electroencephalogr. Clin. Neurophysiol.* 22: 159–166, 1967.
72. FROST, D. O., AND V. S. CAVINESS, JR. Radial organization of thalamic projections to the neocortex of the mouse. *J. Comp. Neurol.* 194: 369–393, 1980.
73. FROST, J. D., JR. EEG-intracellular potential relationship in isolated cerebral cortex. *Electroencephalogr. Clin. Neurophysiol.* 24: 434–443, 1968.
74. FUKADA, Y., AND H. SAITO. The relationship between response characteristics to flicker stimulation and receptive field organization in the cat's optic nerve fibers. *Vision Res.* 11: 227–240, 1971.
75. FUKADA, Y., AND J. STONE. Evidence of differential inhibitory influences on X- and Y-type relay cells in the eat's lateral geniculate nucleus. *Brain Res.* 113: 188–196, 1976.
76. FUSTER, J. M., AND R. F. DOCTER. Variations of optic evoked potentials as a function of reticular activity in rabbits with chronically implanted electrodes. *J. Neurophysiol.* 25: 324–336, 1962.
77. GALAMBOS, R., AND S. A. HILLYARD. Electrophysiological approaches to human cognitive processing. *Neurosci. Res. Program Bull.* 20: 145–265, 1981.
78. GALINDO, A. GABA-picrotoxin interaction in the mammalian central nervous system. *Brain Res.* 14: 763–767, 1969.
79. GALLETTI, C., M. G. MAIOLI, S. SQUATRITO, AND E. RIVA SANSEVERINO. Single unit responses to visual stimuli in cat cortical areas 17 and 18. I. Responses to stationary stimuli of variable intensity. *Arch. Ital. Biol.* 117: 208–230, 1979.
80. GALLETTI, C., S. SQUATRITO, M. G. MAIOLI, AND E. RIVA SANSEVERINO. Single unit responses to visual

stimuli in cat cortical areas 17 and 18. II. Responses to stationary stimuli of variable duration. *Arch. Ital. Biol.* 117: 231–247, 1979.

81. GARDNER-MEDWIN, A. R. Membrane transport and solute migration affecting the brain cell microenvironment. *Neurosci. Res. Program Bull.* 18: 208–226, 1980.
82. GAREY, L. J., E. G. JONES, AND T. P. S. POWELL. Interrelationships of striate and extrastriate cortex with the primary relay sites of the visual pathway. *J. Neurol. Neurosurg. Psychiatry* 31: 135–157, 1968.
83. GAREY, L. J., AND T. P. S. POWELL. The projection of the lateral geniculate nucleus upon the cortex in the cat. *Proc. R. Soc. London Ser. B* 169: 107–126, 1967.
84. GAREY, L. J., AND T. P. S. POWELL. An experimental study of the termination of the lateral geniculo-cortical pathway in the cat and monkey. *Proc. R. Soc. London Ser. B* 179: 41–63, 1971.
85. GEISERT, E. E., JR. Cortical projections of the lateral geniculate nucleus in the cat. *J. Comp. Neurol.* 190: 793–812, 1980.
86. GILBERT, C. D. Laminar differences in receptive field properties of cells in primary visual cortex. *J. Physiol. London* 268: 391–421, 1977.
87. GILBERT, C. D., AND J. P. KELLY. The projections of cells in different layers of the cat's visual cortex. *J. Comp. Neurol.* 163: 81–106, 1975.
88. GILBERT, C. D., AND T. N. WIESEL. Morphology and intracortical projections of functionally characterised neurones in the cat visual cortex. *Nature London* 280: 120–125, 1979.
89. GILBERT, C. D., AND T. N. WIESEL. Clustered intrinsic connections in cat visual cortex. *Neuroscience* 3: 1116–1133, 1983.
90. GINSBURG, A. P. Psychological correlates of a model of the human visual system. *IEEE Trans. Aerosp. Electron. Syst.*: 283–290, 1971. (Proc. 1971 Natl. Aerosp. Electronics Conf.)
91. GLENN, L. L., J. HADA, J. P. ROY, M. DECHÊNES, AND M. STERIADE. Anterograde tracer and field potential analysis of the neocortical layer I projection from nucleus ventralis medialis of the thalamus in cat. *Neuroscience* 7: 1861–1877, 1982.
92. GOLDRING, S., J. S. O'LEARY, T. G. HOLMES, AND M. J. JERVA. Direct response of isolated cerebral cortex of cat. *J. Neurophysiol.* 24: 633–650, 1961.
93. GOTTLIEB, D. I., AND W. M. COWAN. On the distribution of axonal terminals containing spheroidal and flattened synaptic vesicles in the hippocampus and dentate gyrus of the rat and cat. *Z. Zellforsch. Mikrosk. Anat.* 129: 413–429, 1972.
94. GRINVALD, A., A. MANKER, AND M. SEGAL. Visualisation of the spread of activity in rat hippocampal slices by voltage-sensitive optical probes. *J. Physiol. London* 333: 269–291, 1982.
95. GROSSMAN, R. G., AND T. L. HAMPTON. Depolarization of cortical glial cells during electrocortical activity. *Brain Res.* 11: 316–324, 1968.
96. GROSSMAN, R. G., L. WHITESIDE, AND T. L. HAMPTON. The time course of evoked depolarization of cortical glial cells. *Brain Res.* 14: 401–415, 1969.
97. GRUNDFEST, H. Synaptic and ephaptic transmission. In: *The Neurosciences*, edited by G. L. Quarton, T. Melnechuck, and F. O. Schmitt. New York: Rockefeller Univ. Press, 1967, p. 353–372.
98. GRÜSSER, O.-J., AND C. RABELO. Reaktionen einzelner retinaler Neurone auf Lichtblitze. I. Einzelblitze und Lichtblitze wechselnder Frequenz. *Pluegers Arch.* 265: 501–525, 1958.
99. GRÜTZNER, A., O.-J. GRÜSSER, AND G. BAUMGARTNER. Reaktionen einzelner Neurone im optischen Cortex der Katze nach elektrischer Reizung des Nervus opticus. *Arch. Psychiatr. Nervenkr.* 197: 377–404, 1958.
100. GUMNIT, R. J., H. MATSUMOTO, AND C. VASCONETTI. DC activity in the depth of an experimental epileptic focus. *Electroencephalogr. Clin. Neurophysiol.* 28: 333–339, 1970.
101. HABERLY, L. B., AND G. M. SHEPHERD. Current density analysis of summed evoked potentials in opossum prepyriform cortex. *J. Neurophysiol.* 36: 789–803, 1973.
102. HABETS, A. M. M. C., F. H. LOPES DA SILVA, AND W. J. MOLLEVANGER. An olfactory input to the hippocampus of the cat: field potential analysis. *Brain Res.* 182: 47–64, 1980.
103. HAGINS, W. A. Electrical signs of information flow in photoreceptors. *Cold Spring Harbor Symp. Quant. Biol.* 30: 403–418, 1965.
104. HAGINS, W. A., R. D. PENN, AND S. YOSHIKAMI. Dark current and photo-current in retinal rods. *Biophys. J.* 10: 380–412, 1970.
105. HAMMOND, P., AND D. M. MACKAY. Differential responsiveness of simple and complex cells in cat striate cortex to visual texture. *Exp. Brain Res.* 30: 275–296, 1977.
106. HARVEY, A. R. Characteristics of corticothalamic neurons in area 17 of the cat. *Neurosci. Lett.* 7: 177–181, 1978.
107. HEINEMANN, U., AND H. D. LUX. Ionic changes during experimentally induced epilepsies. In: *Progress in Epilepsy*, edited by F. C. Rose. London: Pitman, 1983, p. 87–103.
108. HERKENHAM, M. Laminar organization of thalamic projections to the rat neocortex. *Science* 207: 532–535, 1980.
109. HERZ, A., O. CREUTZFELDT, AND J. FUSTER. Statistische Eigenschaften der Neuronaktivität im ascendierenden visuellen System. *Kybernetik* 2: 61–71, 1964.
110. HODGKIN, A. L., AND A. F. HUXLEY. A quantitative description of membrane currents and its application to conduction and excitation in nerve. *J. Physiol. London* 117: 500–544, 1952.
111. HOELTZELL, P. B., AND R. W. DYKES. Conductivity in the somatosensory cortex of the cat—evidence for cortical anisotropy. *Brain Res.* 177: 61–82, 1979.
112. HOELTZELL, P. B., AND R. W. DYKES. Current source density analysis of the somatosensory evoked potential in the cat. *Soc. Neurosci. Abstr.* 8: 925, 1982.
113. HOFFMANN, K.-P., AND J. STONE. Conduction velocity of afferents to cat visual cortex: a correlation with cortical receptive field properties. *Brain Res.* 32: 460–466, 1971.
114. HOLLÄNDER, H., AND H. VANEGAS. The projection from the lateral geniculate nucleus onto the visual cortex in the cat. *J. Comp. Neurol.* 173: 519–536, 1977.
115. HOLMES, O., AND A. D. SHORT. Interaction of cortical evoked potentials in the rat. *J. Physiol. London* 209: 433–452, 1970.
116. HOLMES, O., AND G. T. SUNDERLAND. Generator sites in acute epileptic foci (abstr.). *Electroencephalogr. Clin. Neurophysiol.* 44: 132, 1978.
117. HORVATH, F. E., AND P. BUSER. Thalamo-caudate-cortical relationships in synchronized activity. I. Differentiation between ventral and dorsal spindle systems. *Brain Res.* 39: 21–41, 1972.
118. HOWLAND, B., J. Y. LETTVIN, W. S. MCCULLOCH, W. PITTS, AND P. D. WALL. Reflex inhibition by dorsal root interaction. *J. Neurophysiol.* 18: 1–17, 1955.

119. HUBEL, D. H., AND T. N. WIESEL. Receptive fields, binocular interaction and functional architecture in the cat's visual cortex. *J. Physiol. London* 160: 106–154, 1962.
120. HUBEL, D. H., AND T. N. WIESEL. Receptive fields and functional architecture in two nonstriate visual areas (18 and 19) of the cat. *J. Neurophysiol.* 28: 229–289, 1965.
121. HUGHES, J. R. Responses from the visual cortex of unanesthetized monkeys. *Int. Rev. Neurobiol.* 7: 99–152, 1965.
122. HUMPHREY, D. R. Re-analysis of the antidromic cortical response. I. Potentials evoked by stimulation of the isolated pyramidal tract. *Electroencephalogr. Clin. Neurophysiol.* 24: 116–129, 1968.
123. HUMPHREY, D. R. Re-analysis of the antidromic cortical response. II. On the contribution of cell discharge and PSPs to the evoked potentials. *Electroencephalogr. Clin. Neurophysiol.* 25: 421–442, 1968.
124. IANSEK, R., AND S. J. REDMAN. An analysis of the cable properties of spinal motoneurones using a brief intracellular current pulse. *J. Physiol. London* 234: 613–636, 1973.
125. IANSEK, R., AND S. J. REDMAN. The amplitude, time course and charge of unitary excitatory post-synaptic potentials evoked in spinal motoneurone dendrites. *J. Physiol. London* 234: 665–688, 1973.
126. JACKSON, J. D. *Classical Electrodynamics*. New York: Wiley, 1975, p. 38–40.
127. JAMI, L. Patterns of cortical population discharges during metrazol-induced seizures in cats. *Electroencephalogr. Clin. Neurophysiol.* 32: 641–654, 1972.
128. JEANNEROD, M., AND K. SAKAI. Occipital and geniculate potentials related to eye movements in unanaesthetized cat. *Brain Res.* 19: 361–377, 1970.
129. JEFFREYS, D. A. The physiological significance of pattern visual evoked potentials. In: *Visual Evoked Potentials in Man: New Developments*, edited by J. E. Desmedt. Oxford, UK: Clarendon, 1977, p. 134–167.
130. JOHN, E. R. Electrophysiological studies of conditioning. In: *The Neurosciences*, edited by G. C. Quarton, T. Melnechuck, and F. O. Schmitt. New York: Rockefeller Univ. Press, 1967, p. 690–704.
131. JOHNSTON, D. Passive cable properties of hippocampal CA3 pyramidal neurons. *Cell Mol. Neurobiol.* 1: 41–55, 1981.
132. JOHNSTON, D., AND T. H. BROWN. Giant synaptic potential hypothesis for epileptic activity. *Science* 211: 294–297, 1981.
133. JONES, E. G. Functional subdivision and synaptic organization of the mammalian thalamus. In: *Neurophysiology IV*, edited by R. Porter. Baltimore, MD: University Park, 1981, vol. 25, 173–245. (Int. Rev. Physiol. Ser.)
134. KARMOS, G., M. MOLNÁR, AND V. CSÉPE. A new multielectrode for chronic recording of intracranial field potentials in the cat. *Physiol. Behav.* 29: 567–571, 1982.
135. KASAMATSU, T. Maintained and evoked unit activity in the mesencephalic reticular formation of the freely moving cat. *Exp. Neurol.* 28: 450–470, 1970.
136. KASAMATSU, T., AND W. R. ADEY. Visual cortical units associated with phasic activity in REM sleep and wakefulness. *Brain Res.* 55: 323–331, 1973.
137. KATCHALSKY, A. K., V. ROWLAND, AND R. BLUMENTHAL. Dynamic patterns of brain cell assemblies. *Neurosci. Res. Program Bull.* 12: 1–187, 1974.
138. KAWAMURA, K. Corticocortical fiber connections of the cat cerebrum. III. The occipital region. *Brain Res.* 51: 41–60, 1973.
139. KLEE, M. R. Different effects on the membrane potential of motor cortex units after thalamic and reticular stimulation. In: *The Thalamus*, edited by D. P. Purpura and M. D. Yahr. New York: Columbia Univ. Press, 1966, p. 287–317.
140. KLEE, M., AND W. RALL. Computed potentials of cortically arranged populations of neurons. *J. Neurophysiol.* 40: 647–666, 1977.

140a. KOMATSU, Y., K. TOYAMA, J. MAEDA, AND H. SAKAGUCHI. Long-term potentiation investigated in a slice preparation of striate cortex of young kittens. *Neurosci. Lett.* 26: 269–274, 1981.

141. KORNACKER, K. Some properties of the afferent pathway in the frog corneal reflex. *Exp. Neurol.* 7: 224–239, 1963.
142. KOSTOPOULOS, G., M. AVOLI, A. PELLEGRINI, AND P. GLOOR. Laminar analysis of spindles and spikes of the spike and wave discharge of feline generalized penicillin epilepsy. *Electroencephalogr. Clin. Neurophysiol.* 53: 1–13, 1982.
143. KRAUT, M. A., J. C. AREZZO, AND H. G. VAUGHAN, JR. A laminar analysis of the cortical flash visual evoked potential in the monkey. *Soc. Neurosci. Abstr.* 9: 1194, 1983.
144. KRNJEVIĆ, K. Chemical nature of synaptic transmission in vertebrates. *Physiol. Rev.* 54: 418–540, 1974.
145. KRNJEVIĆ, K., M. RANDIĆ, AND D. W. STAUGHAN. Nature of a cortical inhibitory process. *J. Physiol. London* 184: 49–77, 1966.
146. KUFFLER, S. W. Discharge patterns and functional organization of mammalian retina. *J. Neurophysiol.* 16: 37–68, 1953.
147. KUHNT, U. Visuelle Reaktionspotentiale an Menschen und Katzen in Abhängigkeit von der Intensität. *Pfluegers Arch.* 298: 82–104, 1967.
148. KULIKOWSKI, J. J. Pattern and movement detection in man and rabbit: separation and comparison of occipital potentials. *Vision Res.* 18: 183–189, 1978.
149. KULIKOWSKI, J. J., P. O. BISHOP, AND H. KATO. Sustained and transient responses by cat striate cells to stationary flashing light and dark bars. *Brain Res.* 170: 362–367, 1979.
150. KUPERSTEIN, M., AND D. WHITTINGTON. A practical 24 channel microelectrode for neural recording in vivo. *IEEE Trans. Biomed. Eng.* 28: 288–293, 1981.
151. KURTZBERG, D., AND H. G. VAUGHAN, JR. Electrophysiologieal observations on the visuomotor system and visual neurosensorium. In: *Visual Evoked Potentials in Man: New Developments*, edited by J. E. Desmedt. Oxford, UK: Clarendon, 1977, p. 314–331.
152. KWAN, H. C., AND J. T. MURPHY. A basis for extracellular current density analysis in cerebellar cortex. *J. Neurophysiol.* 37: 170–180, 1974.
153. KWAN, H. C., AND J. T. MURPHY. Extracellular current density analysis of responses in cerebellar cortex to climbing fiber activation. *J. Neurophysiol.* 37: 333–345, 1974.
154. KWAN, H. C., AND J. T. MURPHY. Extracellular current density analysis of responses in cerebellar cortex to mossy fiber activation. *J. Neurophysiol.* 37: 947–953, 1974.
155. LANDAU, W. M. Analysis of electrical response to antidromic pyramidal tract stimulation in the cat. *Electroencephalogr. Clin. Neurophysiol.* 8: 445–456, 1956.
156. LANDAU, W. M. Evoked potentials. In: *The Neurosciences*, edited by G. L. Quarton, T. Melnechuck, and F. O. Schmitt. New York: Rockefeller Univ. Press, 1967, p. 469–482.
157. LANDAU, W. M., AND M. H. CLARE. A note on the char-

acteristic response pattern in primary sensory projection cortex of the cat following a synchronous afferent volley. *Electroencephalogr. Clin. Neurophysiol.* 8: 457–464, 1956.
158. LAUFER, M., AND M. VERZEANO. Periodic activity in the visual system of the cat. *Vision Res.* 7: 215–229, 1967.
159. LENNIE, P. Parallel visual pathways: a review. *Vision Res.* 20: 561–594, 1980.
160. LETTVIN, J. Y., H. R. MATURANA, W. S. MCCULLOCH, AND W. H. PITTS. What the frog's eye tells the frog's brain. *Proc. Inst. Radio Eng.* 47: 1940–1951, 1959.
161. LEUNG, L. S. Potentials evoked by alvear tract in hippocampal CA1 region of rats. II. Spatial field analysis. *J. Neurophysiol.* 42: 1571–1589, 1979.
162. LEVAY, S., AND D. FERSTER. Relay cell classes in the lateral geniculate nucleus of the cat and the effect of visual deprivation. *J. Comp. Neurol.* 172: 563–584, 1977.
163. LEVAY, S., AND C. D. GILBERT. Laminar patterns of geniculo cortical projection in the cat. *Brain Res.* 113: 1–19, 1976.
164. LEVENTHAL, A. G. Evidence that the different classes of relay cells of cat's lateral geniculate nucleus terminate in different layers of the striate cortex. *Exp. Brain Res.* 37: 349–372, 1979.
165. LEVENTHAL, A. G., AND H. V. B. HIRSCH. Receptive-field properties of neurons in different laminae of visual cortex of the cat. *J. Neurophysiol.* 41: 948–962, 1978.
166. LEVONIAN, E. Evoked potential in relation to subsequent alpha frequency. *Science* 152: 1280–1282, 1966.
167. LI, C.-L., AND S. N. CHOU. Cortical intracellular synaptic potentials and direct cortical stimulation. *J. Cell. Comp. Physiol.* 60: 1–16, 1962.
168. LI, C.-L., C. CULLEN, AND H. H. JASPER. Laminar microelectrode studies of specific somatosensory cortical potentials. *J. Neurophysiol.* 19: 111–130, 1956.
169. LI, C.-L., C. CULLEN, AND H. H. JASPER. Laminar microelectrode analysis of cortical unspecific recruiting responses and spontaneous rhythms. *J. Neurophysiol.* 19: 131–143, 1956.
170. LIVINGSTONE, M. S., AND D. H. HUBEL. Effects of sleep and arousal on the processing of visual information in the cat. *Nature London* 291: 554–561, 1981.
171. LLINÁS, R., AND H. JAHNSEN. Electrophysiology of mammalian thalamic neurones in vitro. *Nature London* 297: 406–408, 1982.
172. LLINÁS, R., AND C. NICHOLSON. Analysis of field potentials in the central nervous system. In: *Handbook of Electroencephalography and Clinical Neurophysiology*, edited by C. F. Stevens. Amsterdam: Elsevier, 1974, vol. 2B, p. 61–83.
173. LLINÁS, R., AND C. NICHOLSON. Reversal properties of climbing fiber potentials in cat Purkinje cells: an example of a distributed synapse. *J. Neurophysiol.* 39: 311–323, 1976.
174. LLINÁS, R., AND M. SUGIMORI. Electrophysiological properties of in vitro Purkinje cell dendrites in mammalian cerebellar slices. *J. Physiol. London* 305: 197–213, 1980.
175. LLINÁS, R., AND Y. YAROM. Properties and distributions of ionic conductances generating electroresponsiveness of mammalian inferior olivary neurones in vitro. *J. Physiol. London* 315: 569–584, 1981.
175a. LOCKTON, J. W., AND O. HOLMES. Penicillin epilepsy in the rat: the responses of different layers of the cortex cerebri. *Brain Res.* 258: 79–89, 1983.
176. LOPES DA SILVA, F. H., A. VAN ROTTERDAM, P. BARTS, E. VAN HEUSDEN, AND W. BURR. Models of neuronal populations: the basic mechanisms of rhythmicity. In: *Progress in Brain Research. Perspectives in Brain Research*, edited by M. A. Corner and D. F. Swaab. Amsterdam: Elsevier, 1976, vol. 45, p. 281–308.
177. LOPES DA SILVA, F. H., AND W. STORM VAN LEEUWEN. The cortical alpha rhythm in dog: the depth and surface profile of phase. *Int. Brain Res. Organ. Monogr. Ser.* 3: 319–333, 1978.
178. LORENTE DE NÓ, R. *A Study of Nerve Physiology. Studies from Rockefeller Inst. Med. Res.* New York: Rockefeller Inst. Med. Res., 1947, vol. 132, pt. II.
179. LUND, J. S., G. H. HENRY, C. L. MACQUEEN, AND A. R. HARVEY. Anatomical organization of the primary visual cortex (area 17) of the cat. A comparison with area 17 of the macaque monkey. *J. Comp. Neurol.* 184: 599–618, 1979.
180. LURIA, A. R. *The Working Brain.* New York: Basic Books, 1973.
181. LUX, H. D. Eigenschaften eines Neuron-Modells mit Dendriten begrenzter Länge. *Pfluegers Arch.* 297: 238–255, 1967.
182. LUX, H. D., AND D. A. POLLEN. Electrical constants of neurons in the motor cortex of the cat. *J. Neurophysiol.* 29: 207–220, 1966.
183. MACKEBEN, M., AND K. NAKAYAMA. Current source density analysis of 16-channel VEP in alert monkey striate cortex suggests extrastriate origin of the surface VEP. *Soc. Neurosci. Abstr.* 9: 1219, 1983.
184. MACLEAN, P. D. The triune brain, emotion and scientific bias. In: *The Neurosciences. Second Study Program*, edited by F. O. Schmitt. New York: Rockefeller Univ. Press, 1970, p. 336–349.
185. MALPELI, J. G. Activity of cells in area 17 of the cat in absence of input from layer A of the lateral geniculate nucleus. *J. Neurophysiol.* 49: 595–610, 1983.
186. MARSHALL, W. H., S. A. TALBOT, AND H. W. ADES. Cortical response of the anesthetized cat to gross photic and electrical afferent stimulation. *J. Neurophysiol.* 6: 1–15, 1943.
186a. MASS, A. M., AND A. YA. SUPIN. Laminar distribution of current sources in the rabbit superior colliculus during optic nerve stimulation. *Neurophysiology* 15: 21–28, 1983.
187. MATSUMOTO, H. Intracellular events during the activation of cortical epileptiform discharges. *Electroencephalogr. Clin. Neurophysiol.* 17: 294–307, 1964.
188. MATSUMOTO, H., AND C. AJMONE MARSAN. Cortical cellular phenomena in experimental epilepsy: interictal manifestations. *Exp. Neurol.* 9: 286–304, 1964.
189. MATSUMOTO, H., AND C. AJMONE MARSAN. Cortical cellular phenomena in experimental epilepsy. Ictal manifestations. *Exp. Neurol.* 9: 305–326, 1964.
190. MEYER, G., AND K. ALBUS. Topography and cortical projections of morphologically identified neurons in the visual thalamus of the cat. *J. Comp. Neurol.* 201: 353–374, 1981.
191. MILLER, R. F., AND J. E. DOWLING. Intracellular responses of the Müller (glial) cells of mudpuppy retina: their relation to b-wave of the electroretinogram. *J. Neurophysiol.* 33: 323–341, 1970.
192. MITZDORF, U. Justification of the assumption of constant resistivity used in current source-density calculations (Appendix). *J. Physiol. London* 304: 216–220, 1980.
193. MITZDORF, U. Qualitative similarity of electrically and visually evoked current source-densities in the cat visual cortex (abstr.). *Pfluegers Arch.* 392: R48, 1982.
194. MITZDORF, U. Visually evoked field potentials and current source-densities in the cat visual cortex (abstr.). *Neurosci. Lett. Suppl.* 14: 256, 1983.
195. MITZDORF, U., AND G. NEUMANN. Effects of monocular

deprivation in the lateral geniculate nucleus of the cat: an analysis of the evoked potentials. *J. Physiol. London* 304: 221–230, 1980.
196. MITZDORF, U., AND W. SINGER. Laminar segregation of afferents to lateral geniculate nucleus of the cat: an analysis of current source density. *J. Neurophysiol.* 40: 1227–1244, 1977.
197. MITZDORF, U., AND SINGER. Prominent excitatory pathways in the cat visual cortex (A 17 and A 18): a current source density analysis of electrically evoked potentials. *Exp. Brain Res.* 33: 371–394, 1978.
198. MITZDORF, U., AND W. SINGER. Excitatory synaptic ensemble properties of the visual cortex of the macaque monkey: a current source density analysis of electrically evoked potentials. *J. Comp. Neurol.* 187: 71–84, 1979.
199. MITZDORF, U., AND W. SINGER. Excitatory synaptic activities of neuronal ensembles in the lateral geniculate nucleus and visual cortex of kittens (abstr.). *Neurosci. Lett. Suppl.* 3: 299, 1979.
200. MITZDORF, U., AND W. SINGER. Monocular activation of visual cortex in normal and monocularly deprived cats: an analysis of evoked potentials. *J. Physiol. London* 304: 203–220, 1980.
201. MOLNÁR, M., G. KARMOS, V. CSÉPE, AND I. WINKLER. Laminar profiles of cortical evoked potentials elicited by stimulation of specific and non-specific afferent structures (abstr.). *Neurosci. Lett. Suppl.* 14: 252, 1983.
202. MOORE, R. Y., AND F. E. BLOOM. Central catecholamine neurone systems: anatomy and physiology of the norepinephrine and epinephrine system. *Annu. Rev. Neurosci.* 2: 113–168, 1979.
203. MORIN, D., AND M. STERIADE. Development from primary to augmenting responses in the somatosensory system. *Brain Res.* 205: 49–66, 1981.
204. MORUZZI, G., AND H. W. MAGOUN. Brain stem reticular formation and activation of the EEG. *Electroencephalogr. Clin. Neurophysiol.* 1: 455–473, 1949.
205. MOUNTCASTLE, V. B. Modality and topographic properties of single neurons of cat's somatic sensory cortex. *J. Neurophysiol.* 20: 408–434, 1957.
206. MOUNTCASTLE, V. B., W. H. TABOT, H. SAKATA, AND J. HYVÄRINEN. Cortical neuronal mechanisms in flutter-vibration studies in unanesthetized monkeys. Neuronal periodicity and frequency discrimination. *J. Neurophysiol.* 32: 452–484, 1969.
207. MOVSHON, J. A., I. D. THOMPSON, AND D. J. TOLHURST. Spatial and temporal contrast sensitivity of neurones in areas 17 and 18 of the cat's visual cortex. *J. Physiol. London* 283: 101–120, 1978.
208. MÜLLER-PREUSS, P., AND U. MITZDORF. Functional anatomy of the inferior colliculus and the auditory cortex: current source density analyses of click-evoked potentials. *Hearing Res.* In press.
209. MUSTARDI, M. J., J. BULLIER, AND G. H. HENRY. Comparison of response properties of three types of monosynaptic S-cell in cat striate cortex. *J. Neurophysiol.* 47: 439–454, 1982.
210. NACIMIENTO, A. C., H. D. LUX, AND O. D. CREUTZFELDT. Postsynaptische Potentiale von Nervenzellen des motorischen Cortex nach elektrischer Reizung spezifischer und unspezifischer Thalamuskerne. *Pfluegers Arch.* 281: 152–169, 1964.
211. NAKAYAMA, K. The relationship of VEP to cortical physiology. *Proc. NY Acad. Sci.* 388: 21–35, 1982.
212. NELSON, P. G., AND H. D. LUX. Some electrical measurements of motoneuron parameters. *Biophys. J.* 10: 55–73, 1970.
213. NEUMANN, G. Intrinsic connectivity in area 18 of the cat. In: *Developmental Neurobiology of Vision*, edited by R. D. Freeman. New York: Plenum, 1979, p. 175–184.
214. NEWMAN, E. A. Current source-density analysis of the b-wave of frog retina. *J. Neurophysiol.* 43: 1355–1366, 1980.
214a. NEWMAN, E. A., Regional specification of retinal glial cell membrane. *Nature London* 309: 155–157, 1984.
215. NEWMAN, E. A., AND L. L. ODETTE. Model of electroretinogram b-wave generation: a test of the K^+ hypothesis. *J. Neurophysiol.* 51: 164–182, 1984.
216. NICHOLSON, C. Theoretical analysis of field potentials in anisotropic ensembles of neuronal elements. *IEEE Trans. Biomed. Eng.* 20: 278–288, 1973.
217. NICHOLSON, C., G. TEN BRUGGENCATE, H. STÖCKLE, AND R. STEINBERG. Calcium and potassium changes in extracellular micro environment of cat cerebellar cortex. *J. Neurophysiol.* 41: 1026–1039, 1978.
218. NICHOLSON, C., AND J. A. FREEMAN. Theory of current source-density analysis and determination of conductivity tensor for anuran cerebellum. *J. Neurophysiol.* 38: 356–368, 1975.
219. NICHOLSON, C., AND R. LLINÁS. Field potentials in the alligator cerebellum and theory of their relationship to Purkinje cell dendritic spikes. *J. Neurophysiol.* 34: 509–531, 1971.
220. NICHOLSON, C., AND R. LLINÁS. Real time current source-density analysis using multi-electrode array in cat cerebellum. *Brain Res.* 100: 413–424, 1975.
221. NICHOLSON, P. W. Specific impedance of cerebral white matter. *Exp. Neurol.* 13: 386–401, 1965.
222. NICOLL, R. A., J. C. ECCLES, T. OSHIMA, AND F. RUBIA. Prolongation of hippocampal postsynaptic potentials by barbiturates. *Nature London* 258: 625–627, 1975.
223. NIIMI, K., AND J. M. SPRAGUE. Thalamo-cortical organization of the visual system in the cat. *J. Comp. Neurol.* 138: 219–250, 1970.
224. OGDEN, T. E., AND H. ITO. Avian retina. II. An evaluation of retinal electrical anisotropy. *J. Neurophysiol.* 34: 367–373, 1971.
225. OREM, J., AND D. M. FEENEY. Reciprocal reticular influences on cells in rostral and caudal visual cortex of the cat. *Brain Res.* 30: 200–203, 1971.
226. ORKAND, R. K. Glial cells. In: *Handbook of Physiology. The Nervous System*, edited by J. M. Brookhart and V. B. Mountcastle. Bethesda, MD: Am. Physiol. Soc., 1977, sect. 1, vol. I, pt. 2, chapt. 23, p. 855–875.
227. OTSUKA, R., AND R. HASSLER. Über Aufbau und Gliederung der corticalen Sehsphäre bei der Katze. *Arch. Psychiatr. Nervenkr.* 203: 212–234, 1962.
228. PALMER, L. A., AND A. C. ROSENQUIST. Visual receptive fields of single striate cortical units projecting to the superior colliculus in the cat. *Brain Res.* 67: 27–42, 1974.
229. PANTLE, A. Motion aftereffect magnitude as a measure of the spatio-temporal response properties of direction-sensitive analyzers. *Vision Res.* 14: 1229–1236, 1974.
230. PERL, E. R., AND D. G. WHITLOCK. Potentials evoked in cerebral somatosensory region. *J. Neurophysiol.* 18: 486–501, 1955.
231. PETSCHE, H., H. POCKBERGER, AND R. RAPPELSBERGER. Current source density study of epileptic phenomena and the morphology of the rabbit's striate cortex. In: *Physiology and Pharmacology of Epileptogenic Phenomena*, edited by M. R. Klee, H. D. Lux, and E. J. Speckmann. New York: Raven, 1982, p. 53–63.
232. PITTS, W. Investigation on synaptic transmission. In: *Cybernetics.* New York: Trans. 9th Conf. Josiah Macy Found., 1952, p. 159–166.

233. PLONSEY, R. *Bioelectric Phenomena.* New York: McGraw-Hill, 1969.
234. POCHAY, P., K. D. WISE, L. F. AILARD, AND L. T. RUTLEDGE. A multichannel depth probe fabricated using electron-beam lithography. *IEEE Trans. Biomed. Eng.* 26: 199–206, 1979.
235. POLLEN, D. A. On the generation of neocortical potentials. In: *Basic Mechanism of Epilepsies,* edited by H. H. Jasper, A. A. Ward, and A. Pope. Boston, MA: Little, Brown, 1969, p. 411–420.
236. POLLEN, D. A., AND H. D. LUX. Conductance changes during inhibitory postsynaptic potentials in normal and strychninized cortical neurons. *J. Neurophysiol.* 29: 369–381, 1966.
237. POLLEN, D. A., K. H. REID, AND P. PEROT. Microelectrode studies of experimental 3/sec wave and spike in the cat. *Electroencephalogr. Clin. Neurophysiol.* 17: 57–67, 1964.
238. PRIBRAM, K. H. *Languages of the Brain.* Englewood Cliffs, NJ: Prentice-Hall, 1971.
239. PRINCE, D. A. Neurophysiology of epilepsy. *Annu. Rev. Neurosci.* 1: 395–415, 1978.
240. PROHASKA, O., F. PACHA, P. PPUNDNER, AND H. PETSCHE. A 16-fold semimicroelectrode for intracortical recording of field potentials. *Electroencephalogr. Clin. Neurophysiol.* 47: 629–631, 1979.
241. PURPURA, D. P. Intracellular studies of synaptic organizations in the mammalian brain. In: *Structure and Function of Synapses,* edited by G. D. Pappas and D. P. Purpura. New York: Raven, 1972, p. 257–302.
242. PURPURA, D. P., AND R. J. SHOFER. Cortical intracellular potentials during augmenting and recruiting responses. I. Effects of injected hyperpolarizing currents on evoked membrane potential changes. *J. Neurophysiol.* 27: 117–132, 1964.
243. PURPURA, D. P., R. J. SHOFER, AND T. SCARFF. Properties of synaptic activities and spike potentials of neurons of immature neocortex. *J. Neurophysiol.* 28: 925–942, 1965.
244. RALL, W. Distinguishing theoretical synaptic potentials computed for different soma-dendritic distributions of synaptic input. *J. Neurophysiol.* 30: 1138–1168, 1967.
245. RALL, W. Time constants and electrotonic length of membrane cylinders and neurons. *Biophys. J.* 9: 1483–1508, 1969.
246. RALL, W. Core conductor theory and cable properties of neurons. In: *Handbook of Physiology. The Nervous System,* edited by J. M. Brookhart and V. B. Mountcastle. Bethesda, MD: Am. Physiol. Soc., 1977, sect. 1, vol. I, pt. 1, chapt. 3, p. 39–97.
247. RANCK, J. B., JR. Specific independance of rabbit cerebral cortex. *Exp. Neurol.* 7: 144–152, 1963.
248. RANCK, J. B., JR., AND S. L. BeMENT. The specific impedance of the dorsal columns of cat: an anisotropic medium. *Exp. Neurol.* 11: 451–463, 1965.
249. RANSOM, B. R., AND S. GOLDRING. Slow depolarization in cells presumed to be glia in cerebral cortex of cat. *J. Neurophysiol.* 36: 869–878, 1973.
250. RANSOM, B. R., AND S. GOLDRING. Slow hyperpolarization in cells presumed to be glia in cerebral cortex of cat. *J. Neurophysiol.* 36: 879–892, 1973.
251. RAPPELSBERGER, P., H. POCKBERGER, AND H. PETSCHE. Current source density analysis: methods and application to simultaneously recorded field potentials of the rabbit's visual cortex. *Pflueqers Arch.* 389: 159–170, 1981.
252. RAPPELSBERGER, P., H. POCKBERGER, AND H. PETSCHE. The contribution of the cortical layers to the generation of the EEG: field potentials and current source density analyses in the rabbit's visual cortex. *Electroencephalogr. Clin. Neurophysiol.* 53: 254–269, 1982.
253. REBERT, C. S. Slow potential correlates of neuronal population responses in the cat lateral geniculate nucleus. *Electroencephalogr. Clin. Neurophysiol.* 35: 511–515, 1973.
254. REDMAN, S. J. A quantitative approach to integrated function of dendrites. In: *Neurophysiology II,* edited by R. Porter. 1976, vol. 10, p. 1–35. (Int. Rev. Physiol. Ser.)
255. RÊMOND, A., AND N. LESÈVRE. Variations in average visual evoked potentials as a function of alpha-rhythm phase. *Electroencephalogr. Clin. Neurophysiol. Suppl.* 26: 42–52, 1967.
256. RIBACK, C. E. Aspinous and sparsely-spinous stellate neurons in the visual cortex of rats containing glutamic acid decarboxylase. *J. Neurocytol.* 7: 461–478, 1978.
257. RIVA SANSEVERINO, E., C. GALLETTI, M. G. MAIOLI, AND S. SQUATRITO. Single unit responses to visual stimuli in cat cortical areas 17 and 18. III. Responses to moving stimuli of variable velocity. *Arch. Ital. Biol.* 117: 248–267, 1979.
258. RIZZOLATTI, G., AND R. CAMARDA. Influence of the presentation of remote visual stimuli on visual responses of cat area 17 and lateral suprasylvian area. *Exp. Brain Res.* 29: 107–122, 1977.
259. ROCKLAND, K. S., AND J. S. LUND. Intrinsic laminar lattice connections in primate visual cortex. *J. Comp. Neurol.* 216: 303–318, 1983.
260. ROSE, D., AND C. BLAKEMORE. Effects of bicuculline on functions of inhibition in visual cortex. *Nature London* 249: 375–377, 1974.
261. ROSEN, R. Hierarchical organization in automata theoretic models of the central nervous system. In: *Information Processing in the Nervous System,* edited by K. N. Leibovic. New York: Springer-Verlag, 1969, p. 21–35.
262. ROSENQUIST, A. C., S. B. EDWARDS, AND L. A. PALMER. An autoradiographic study of the projections of the dorsal lateral geniculate nucleus and the posterior nucleus in the cat. *Brain Res.* 80: 71–93, 1974.
263. ROSSIGNOL, S., AND M. COLONNIER. A light microscope study of degeneration patterns in cat cortex after lesions of the lateral geniculate nucleus. *Vision Res. Suppl.* 3: 329–338, 1971.
264. ROWE, M. H., AND J. STONE. Conduction velocity groupings among axons of cat retinal ganglion cells, and their relationship to retinal topography. *Exp. Brain Res.* 25: 339–357, 1976.
265. SAKHIULINA, G. T., AND G. K. MERZHANOVA. Stable changes in the pattern of the recruiting response associated with a well established conditioned reflex. *Electroencephalogr. Clin. Neurophysiol.* 20: 50–58, 1966.
266. SANIDES, F. Functional architecture of motor and sensory cortices in the light of a new concept of neocortex evolution. In: *The Primate Brain,* edited by C. Noback and W. Montagna. New York: Appleton-Century-Crofts, 1970, p. 137–208.
267. SATOH, T. Direct cortical response and PGO spike during paradoxical sleep of the cat. *Brain Res.* 28: 576–578, 1971.
268. SCHAUL, N., P. GLOOR, G. BALL, AND J. GOTMAN. The electromicrophysiology of delta waves induced by systemic atropine. *Brain Res.* 143: 475–486, 1978.
269. SCHEIBEL, M. E., AND A. B. SCHEIBEL. Elementary processes in selected thalamic and cortical subsystems—the structural substrates. In: *The Neurosciences. Second Study Program,* edited by F. O. Schmitt. New York: Rockefeller Univ. Press, 1970, p. 443–457.
270. SCHERRER, J. Organization of spontaneous electrical activity in the neocortex. In: *Progress in Brain Research. Perspectives in Brain Research,* edited by M. A. Corner and D. F. Swaab. Amsterdam: Elsevier, 1976, vol. 45, p. 309–325.
271. SCHMIELAU, F., AND W. SINGER. The role of visual cortex for binocular interaction in the cat lateral geniculate nucleus. *Brain Res.* 120: 354–361, 1977.
272. SCHUBERT, P., AND U. MITZDORF. Analysis and quantitative evaluation of the depressive effect of adenosine on evoked potentials in hippocampal slices. *Brain Res.* 172: 186–190, 1979.
273. SIERRA, G., AND J. M. FUSTER. Facilitation of secondary visual evoked responses by stimulation of limbic structures. *Electroencephalogr. Clin. Neurophysiol.* 25: 274–278, 1968.
274. SIESJÖ, B. K., AND M. INGVAR. Blood flow. In: *Handbook of Neurochemistry,* edited by A. Lajtha. New York: Plenum, 1983, vol. 3, p. 653–688.
275. SILLITO, A. M. Inhibitory mechanisms influencing complex cell orientation selectivity and their modification at high resting discharge levels. *J. Physiol. London* 289: 33–53, 1979.
276. SINGER, W. The effect of mesencephalic reticular stimulation on intracellular potentials of cat lateral geniculate neurons. *Brain Res.* 61: 35–54, 1973.
277. SINGER, W. Central core control of developmental plasticity in the kitten visual cortex. I. Diencephalic lesions. *Exp. Brain Res.* 47: 209–222, 1982.
278. SINGER, W., M. VON GRÜNAU, AND J. RAUSCHECKER. Functional amblyopia in kittens with unilateral exotropia. I. Electrophysiological assessment. *Exp. Brain Res.* 40: 294–304, 1980.
279. SINGER, W., F. TRETTER, AND M. CYNADER. Organization of cat striate cortex: a correlation of receptive-field properties with afferent and efferent connections. *J. Neurophysiol.* 38: 1080–1098, 1975.
280. SINGER, W., F. TRETTER, AND M. CYNADER. The effect of reticular stimulation on spontaneous and evoked activity in the cat visual cortex. *Brain Res.* 102: 71–90, 1976.
281. SKREBITSKY, V. G., AND I. N. SHARONOVA. Reticular suppression of flash-evoked IPSPs in visual cortex neurons. *Brain Res.* 111: 67–78, 1976.
282. SNYDER, M., AND I. T. DIAMOND. The organization and function of the visual cortex in the tree shrew. *Brain Behav. Evol.* 1: 244–288, 1968.
283. SOKOLOFF, L. The relationship between function and energy metabolism: its use in the localization of functional activity in the nervous system. *Neurosci. Res. Program Bull.* 19: 159–210, 1980.
284. SOMOGYI, P. The study of Golgi stained cells and of experimental degeneration under the electron microscope: a direct method for the identification in the visual cortex of three successive links in a neuron chain. *Neuroscience* 3: 167–180, 1978.
285. SOMOGYI, P., T. F. FREUND, J.-Y., WU, AND A. D. SMITH. The section-Golgi procedure. 2. Immunocytochemical demonstration of glutamate decarboxylase in Golgi-impregnated neurons and their afferent synaptic boutons in the visual cortex of the cat. *Neuroscience* 9: 475–490, 1983.
286. SPENCER, W. A., AND J. M. BROOKHART. Electrical patterns of augmenting and recruiting waves in depths of sensorimotor cortex of cat. *J. Neurophysiol.* 24: 26–49, 1961.
287. SPENCER, W. A., AND J. M. BROOKHART. A study of spontaneous spindle waves in sensorimotor cortex of cat. *J. Neurophysiol.* 24: 50–65, 1961.
288. SPERRY, R. W. A modified concept of consciousness. *Psychol. Rev.* 76: 532–536, 1969.
289. STERIADE, M. Interneuronal epileptic discharges related to spike-and-wave cortical seizures in behaving monkeys. *Electroencephalogr. Clin. Neurophysiol.* 37: 247–263, 1974.
290. STERIADE, M. Mechanisms underlying cortical activation: neuronal organization and properties of the midbrain reticular core and intralaminar thalamic nuclei. In: *Brain Mechanisms of Perceptual Awareness and Purposeful Behavior,* edited by O. Pompeiano and C. Ajmone Marsan. New York: Raven, 1981, p. 327–378.
291. STERIADE, M., AND D. MORIN. Reticular influences on primary and augmenting responses in the somatosensory cortex. *Brain Res.* 205: 67–80, 1981.
292. STERIADE, M., N. ROPERT, A. KITSIKIS, AND G. OAKSON. Ascending activating neuronal networks in midbrain reticular core and related rostral systems. In: *The Reticular Formation Revisited,* edited by J. A. Hobson and M. A. B. Brazier. New York: Raven, 1980, p. 125–167.
293. STONE, J. Sampling properties of microelectrodes assessed in the cat's retina. *J. Neurophysiol.* 36: 1071–1079, 1973.
294. STONE, J., AND B. DREHER. Projection of X- and Y-cells of the cat's lateral geniculate nucleus to areas 17 and 18 of visual cortex. *J. Neurophysiol.* 36: 551–567, 1973.
295. STONE, J., AND J. A. FREEMAN. Synaptic organization of the pigeon's optic tectum: a Golgi and current source-density analysis. *Brain Res.* 27: 203–221, 1971.
296. STRICK, P. L., AND P. STERLING. Synaptic termination of afferents from the ventrolateral nucleus of the thalamus in the cat motor cortex. A light and electron microscope study. *J. Comp. Neurol.* 153: 77–106, 1974.
297. SUZUKI, T. A., S. NUNOKAWA, AND J. H. JACOBSON. Visually evoked cortical response in light-adapted cat and liminal brightness discrimination. *Jpn. J. Physiol.* 22: 157–175, 1972.
298. SZENTÁGOTHAI, J. Synaptology of the visual cortex. In: *Handbook of Sensory Physiology. Visual Centers in the Brain,* edited by R. Jung. Berlin: Springer-Verlag, 1973, vol. VII, pt. 3/B, p. 269–324.
299. SZENTÁGOTHAI, J. The neuron network for the cerebral cortex: a functional interpretation. *Proc. R. Soc. London Ser. B* 201: 219–248, 1978.
300. SZERB, J. C. Averaged evoked potentials and cholinergic synapses in the somatosensory cortex of the cat. *Electroencephalogr. Clin. Neurophysiol.* 18: 140–146, 1965.
301. TAKAHASHI, K., K. KUBOTA, AND M. UNO. Recurrent facilitation in cat pyramidal tract cells. *J. Neurophysiol.* 30: 22–34, 1967.
302. TANAKA, K. Cross-correlation analysis of geniculostriate neuronal relationships in cats. *J. Neurophysiol.* 49: 1303–1318, 1983.
303. TERZUOLO, C. A., AND T. ARAKI. An analysis of intra- versus extracellular potential changes associated with activity of single spinal motoneurons. *Ann. NY Acad. Sci.* 94: 547–558, 1961.
304. TORRES, F., AND J. S. WARNER. Some characteristics of delayed responses to photic stimuli in the cat. *Electroencephalogr. Clin. Neurophysiol.* 14: 654–663, 1962.
305. TOWE, A. L. On the nature of the primary evoked response. *Exp. Neurol.* 15: 113–139, 1966.
306. TOWE, A. L., M. D. MANN, AND G. W. HARDING. On the currents that flow during the strychnine spike. *Electroencephalogr. Clin. Neurophysiol.* 51: 306–327, 1981.
307. TOYAMA, K., K. MATSUNAMI, T. OHNO, AND S. TOKASHIKI. An intracellular study of neuronal organization in the visual cortex. *Exp. Brain Res.* 21: 45–66, 1974.
308. TRETTER, F., M. CYNADER, AND W. SINGER. Cat par-

astriate cortex: a primary or secondary visual area? *J. Neurophysiol.* 38: 1099–1113, 1975.

309. TSUMOTO, T., W. ECKART, AND O. D. CREUTZFELDT. Modification of orientation sensitivity of cat visual cortex neurons by removal of GABA-mediated inhibition. *Exp. Brain Res.* 34: 351–363, 1979.
310. TUSA, R. J., L. A. PALMER, AND A. C. ROSENQUIST. The retinotopic organization of area 17 (striate cortex) in the cat. *J. Comp. Neurol.* 177: 213–236, 1978.
311. TUSA, R. J., A. C. ROSENQUIST, AND L. A. PALMER. Retinotopic organization of areas 18 and 19 in the cat. *J. Comp. Neurol.* 185: 657–678, 1979.
312. VANEGAS, H., E. ESSAYAG-MILLÁN, AND M. LAUFER. Response of the optic tectum to stimulation of the optic nerve in the teleost *Eugerres plumieri*. *Brain Res.* 31: 107–118, 1971.
313. VANEGAS, H., B. WILLIAMS, AND J. A. FREEMAN. Responses to stimulation of marginal fibers in the teleostean optic tectum. *Exp. Brain Res.* 34: 335–349, 1979.
314. VAUGHAN, H. G., JR. *Neurosci. Res. Program Bull.* 20: 218, 1981.
315. VAUGHAN, H. G., JR., AND C. G. GROSS. Cortical responses to light in unanesthetized monkeys and their alteration by visual system lesions. *Exp. Brain Res.* 8: 19–36, 1969.
316. WACHTMEISTER, L., AND J. E. DOWLING. The oscillatory potentials in the mudpuppy retina. *Invest. Ophthalmol. Vis. Sci.* 17: 1176–1188, 1978.
317. WADMAN, W. J., B. MELCHERS, AND F. H. LOPES DA SILVA. Analysis of field potential profiles during long term potentiation in dentate gyrus slices from the rat (abstr.). *Neurosci. Lett. Suppl.* 14: 396, 1983.
318. WATANABE, S., M. KONISHI, AND O. D. CREUTZFELDT. Postsynaptic potentials in the cat's visual cortex following electrical stimulation of afferent pathways. *Exp. Brain Res.* 1: 272–283, 1966.
319. WHITTAKER, S. G., AND J. B. SIEGFRIED. Origin of wavelets in the visual evoked potential. *Electroencephalogr. Clin. Neurophysiol.* 55: 91–101, 1983.
320. WIDÉN, L., AND C. AJMONE MARSAN. Unitary analysis of the response elicited in the visual cortex of cat. *Arch. Ital. Biol.* 98: 248–274, 1960.
321. WILSON, J. T. L., AND W. SINGER. Simultaneous visual events show a long-range spatial interaction. *Percept. Psychophys.* 30: 107–113, 1981.
322. WILSON, M. E. Cortico-cortical connexions of the cat visual areas. *J. Anat.* 102: 375–386, 1968.
323. WONG, R. K. S., D. A. PRINCE, AND A. I. BASBAUM. Intradendritic recordings from hippocampal neurons. *Proc. Natl. Acad. Sci. USA* 76: 986–990, 1979.
324. YEDLIN, M., H. KWAN, J. T. MURPHY, H. NGUYEN-HUU, AND Y. C. WONG. Electrical conductivity in cat cerebellar cortex. *Exp. Neurol.* 43: 556–569, 1974.

PHYSIOLOGICAL REVIEWS
Vol. 65, No. 1, January 1985
Printed in U.S.A.

Effect of Anoxia on Ion Distribution in the Brain

ANKER JON HANSEN

Institute of Medical Physiology, Department A, University of Copenhagen, Copenhagen, Denmark

1. INTRODUCTION

The function of the mammalian brain depends on a continuous supply of O_2 and glucose. When the brain no longer receives either of these substances, loss of function occurs quickly (83, 254), and viability is endangered when the lack of substrates persists for more than a few minutes (51, 83). These special conditions, which are not found in any other organ, present an important pathophysiological and clinical problem.

0031-9333/85 $1.50 Copyright © 1985 the American Physiological Society